Author's response to referee #1

Thank you for your helpful comments. We revised the manuscript based on your comments and suggestions.

In this study, the authors implement a brown carbon scheme into a global model, evaluate a series of simulations with varying assumptions about photobleaching and convective transport against observations from HIPPO, SEAC4RS and DC3, and then estimate the heating rates and DREs from their simulation which best fits observations. This is certainly an interesting topic which warrants further modeling studies to explore the impacts of large uncertainties in our understanding of the properties and evolution of BrC in the atmosphere. There are however two major issues in this manuscript that should be addressed prior to publication (as well as more minor issues described below):

Author's response: Thank you for your suggestions. The point-by-point responses to your questions and comments are presented below.

1. This modeling study shares significant methodological overlap with previous modeling efforts for BrC, particularly Wang et al, ACP, 2018 and Brown et al., ACP, 2018, the first of which compares to the same BrC observations used here and the second of which uses the same model. Both of these previous model studies explore photobleaching. The primary novelty of this study is therefore the focus on convective transport. The authors should therefore be careful not to overstate the novelty of their work, and acknowledge and contrast to the existing literature throughout (Introduction, Results, Conclusions), particularly how assumptions made in this study might differ from these previous studies, why different assumptions might have been implemented, and how this impacts the comparison with these previous studies.

Author's response: In the revised manuscript, we clarified the differences of our simulations of BrC from previous studies. The implementation of BrC photo-bleaching in Wang et al (2018) and Brown et al (2018) specified a uniform 1-day e-folding time for BrC, and BrC bleaching rate, depending on OH concentrations, until 25% of the original BrC absorption is left. Our approach to BrC photobleaching considers the bleaching effects from different sources. We specify a decay half-life of 12 hours when light is present for primary biomass and biofuel BrC in the daytime until 6% is left and no further photobleaching occurs (Forrister et al., 2015). The half-life for secondary aromatic BrC is specified at 12 hours in daytime (Liu et al., 2016). The revised text is added in Lines 164-177: "Previous modeling of the BrC photo-bleaching effect by Wang et al. (2018) and Brown et al. (2018) applied a 1-day e-folding time for BrC before reaching a threshold of 25% of the original BrC absorption. Our approach to BrC photo-bleaching considers different bleaching effects depending on BrC source. We specify a decay half-life of 12 hours when light is present for primary biomass and biofuel BrC in the daytime until 6% is left and no further photo-bleaching occurs (Forrister et al., 2015) due to stable high molecular weight chromophores (Di Lorenzo and Young, 2015; Di Lorenzo et al., 2017; Wong et al., 2017; Wong et al, 2019). Different components of SOA have different photo-bleaching lifetimes. Aromatic SOA has a half-life of 12-24 hours (Liu et al., 2016; Lee et al., 2014; Zhong and Jang, 2011), limonene SOA has a half-life of <0.5 hours (Lee et al., 2014). Methylglyoxal SOA has a half-life of 90 minutes (Zhao et al., 2015; Wong et al., 2017). Therefore, the half-life for secondary aromatic BrC is specified at 12 hours in daytime until it is completely removed (Liu et al., 2016)."

In Lines 389-393, we added: "The 0.013 W/m^2 DRE in the NCB simulation is lower than previous model studies considering the photo-bleaching effect (Wang et al., 2018; Brown et al., 2018). In the NCB simulation, remote BrC concentrations are mostly affected by the lower threshold for photo-bleaching, which is 6% in this study (Forrister et al. 2015) in comparison to 25% in Wang et al. (2018)

and Brown et al. (2018), causing the difference in the global DRE estimates with photo-bleaching between this work and previous studies.

In the introduction section, Lines 82-83, we added "Model simulation results without considering the differential convective transport and BC and BrC are compared to previous studies."

In the conclusions section, Lines 441-443, we added "Compared to previous studies which did not consider differential convective transport of BrC and BC, the simulated BrC DREs without (NCNB) and with (NCB) photo-bleaching are comparable to previous studies (Feng et al., 2013; Jo et al., 2016; Wang et al., 2018; Brown et al., 2018)."

2. While the heating rate conclusions are the most interesting aspect of the manuscript, the results are substantially overstated. Figure 13 shows that BrC heating rates barely exceed those of BC in the UT in convective regions. Given that uncertainties on the simulation (convective parameterization, removal, optical properties, etc, etc, etc) are large, the authors cannot state with high confidence that the heating rate from BrC exceeds BC. In particular, given that this study does not include any observational evaluation in the tropics, where the authors suggest this effect is most important, this conclusion is unsupported. The authors should temper the discussion of these results. Similarly, the manuscript title should be modified to eliminate overstatement of the results.

Author's response: We agree with the reviewer that the uncertainties of BrC module may lead to biases in the simulated BrC heating over the upper troposphere. We updated the title to "*Modeling global radiative effect of brown carbon: A potentially larger heating source in the tropical free troposphere than black carbon*" and add more discussion in Conclusion section admitting the uncertainties of the BrC parameterization.

In the conclusion section, Lines 461-464, we emphasized the uncertainties: "There are still considerable uncertainties in modeling BrC absorption and its effects in the atmosphere. Parameterizations of emissions, photo-bleaching, and convective transport of BrC all require more field and laboratory observations. The modeling result of stronger atmospheric heating by BrC than BC over the tropical free troposphere in this study are subject to these uncertainties. Field measurements over tropical convective regions during periods of biomass burning are critically needed to further improve our understanding of BrC processes and its climate effects…"

Additional comments

1. Line 70: missing name on reference

Author's response: Thank you for pointing out. Reference added on line 70 (now line 73).

2. Lines 91-95: specify meteorological years simulated

Author's response: Our free-running simulations are based on the climatology of 2010. We updated this in line 101.

3. Section 2.2: Should discuss how many different emission factors (i.e. biomes) are used in the inventory and whether their resulting BrC inventory adequately represents the variability in fuels.

Author's response: We updated the emission factor variability in the page 4, lines 117-119 "The

different emission factors for tropical forest, temperate forest, boreal forest, savanna, agriculture waste and peat burning are based on Akagi et al. (2011)." We added "The variability of BrC emission rate among biomes therefore depends on the BC to OA emission ratios in the GFED emission inventory." in page 7, lines 208-209.

4. Section 2.2: Given that the authors rely on comparisons between BrC and BC later in the text, they should include details on BC aging and optical properties in this section.

Author's response: We added the information at the end of section 2, lines 133-135.

5. Lines 130 and 133: use the same wavelength for MAEs so that they can be compared

Author's response: We updated MAEs in the same wavelength in line 144. The MAE value at 550 nm for secondary BrC is 0.19 m^2/g in the model.

6. Line 203-204: specify that this statement applies to the default model

Author's response: We updated that this statement applies to the default model and all sensitivity runs at lines 241-242.

7. Lines 199-215: discussion of BC removal should also reference and compare to approach of global model study of Q. Wang et al. (JGR, 2014).

Author's response: Wang et al. (2014) updated the model wet scavenging by scavenging hydrophobic aerosols in convective updrafts and scavenging hydrophilic aerosols from cold clouds. We increased the interstitial BC scavenging by a factor of 5 to increase wet scavenging and reduced stratiform liquid-containing cloud based on model evaluations using HIPPO data. We updated this in Page 8, Lines 240-244.

8. Line 243: requires citation at the end of the sentence.

Author's response: We moved the citation to the end of the sentence.

9. Lines 245-252: it would be useful to discuss why BrC scavenging isn't treated similarly to BC scavenging in each simulation

Author's response: We updated the wet scavenging efficiency of BrC based on the convection outflow/inflow ratio discussed in Zhang et al. (2017).

10. Figure 7: Why don't the authors compare observed and simulated OA mass and BrC absorption directly?

Author's response: We updated the comparison of BrC between the model results and observations in the supplement. The change of BrC/BC indicates the different physical chemical properties between BrC and BC, so the ratio of BrC to BC is an important factor when estimating the physical chemical properties of BrC. In figure 7, we compared BrC/BC between the model and the observation.

11. Line 262: "During DC3 experiment, respectively." Is not a sentence

Author's response: We changed the typo in the updated manuscript.

12. Line 263: "Both the observations and model simulations show the increase of BrC/BC ratio at in the upper troposphere"; statement is inaccurate, model simulations do not show increase.

Author's response: The sentence is removed.

13. Lines 261-284: This discussion is a little confusing. It should be clear from the text that the NCB and ICNB simulations are inconsistent with observations, but also that no model simulation captures the

increase in BrC/BC as observed, particularly for SEAC4RS.

Author's response: In section 5.1, lines 319-321, we showed in the text that NCB simulation underestimated the BrC/BC ratio in both DC-3 and SEAC^{4}RS, and ICNB overestimated the BrC/BC ratio in the observations. In lines 325-326, we now acknowledged that no model simulation captured the increase in BrC/BC as observed in SEAC4RS.

14. Line 314: I think the authors mean DRE not "radiative forcing" here to be consistent with their earlier discussion.

Author's response: Corrected. Thank you.

Brown, H., Liu, X., Feng, Y., Jiang, Y., Wu, M., Lu, Z., Wu, C., Murphy, S. and Pokhrel, R., 2018. Radiative effect and climate impacts of brown carbon with the Community Atmosphere Model (CAM5). Atmospheric Chemistry and Physics, 18, 17745-17768, https://doi.org/10.5194/acp-18-17745-2018, 2018.

Forrister, H., Liu, J., Scheuer, E., Dibb, J., Ziemba, L., Thornhill, K. L., Anderson, B., Diskin, G., Perring, A. E., and Schwarz, J. P.: Evolution of brown carbon in wildfire plumes, Geophysical Research Letters, 42, 4623-4630, https://doi.org/10.1002/2015GL063897, 2015.

Liu, J., Lin, P., Laskin, A., Laskin, J., Kathmann, S. M., Wise, M., Caylor, R., Imholt, F., Selimovic, V., and Shilling, J. E.: Optical properties and aging of light-absorbing secondary organic aerosol, Atmospheric Chemistry and Physics, 16, 12815-12827, https://doi.org/10.5194/acp-16-12815-2016, 2016.

Wang, Q., Jacob, D.J., Spackman, J.R., Perring, A.E., Schwarz, J.P., Moteki, N., Marais, E.A., Ge, C., Wang, J. and Barrett, S.R.: Global budget and radiative forcing of black carbon aerosol: Constraints from pole-to-pole (HIPPO) observations across the Pacific. Journal of Geophysical Research: Atmospheres, 119(1), pp.195-206, https://doi.org/10.1002/2013JD020824, 2013.

Wang, X., Heald, C. L., Liu, J., Weber, R. J., Campuzano-Jost, P., Jimenez, J. L., Schwarz, J. P., and Perring, A. E.: Exploring the observational constraints on the simulation of brown carbon, Atmospheric Chemistry and Physics, 18, 635, https://doi.org/10.5194/acp-18-635-2018, 2018.

Zhang, Y., Forrister, H., Liu, J., Dibb, J., Anderson, B., Schwarz, J. P., Perring, A. E., Jimenez, J. L., Campuzano-Jost, P., and Wang, Y.: Top-of-atmosphere radiative forcing affected by brown carbon in the upper troposphere, Nature Geoscience, 10, 486, https://doi.org/10.1038/ngeo2960, 2017.

Author's response to referee #2

Thank you for your helpful comments. We response to your comments and revise the manuscript based on the comments, described in the following content.

This study examines the global direct radiative effect of brown carbon (BrC), using the Community Atmospheric Model version 5 (CAM5). A biomass burning emission inventory and aerosol module for BrC are developed and implemented into CAM5. The direct radiative effect (DRE) due to BrC absorption is estimated, and the results show that the atmospheric heating by BrC is the most significant in the mid and upper troposphere over the tropics, exceeding the BC heating effect. Sensitivity studies are conducted to demonstrate the relative importance of the BrC photo-bleaching effect and convective wet scavenging on the estimated BrC DREs. Overall, this study presents interesting findings about the global distributions of BrC and its radiative effects relative to black carbon (BC). However, there are some major concerns about the modeling approach that need to be addressed before consideration for publication.

Author's response: Thank you for your suggestions. The point-by-point responses to your questions and comments are presented below.

First, the parameterization of BrC needs clarification and justification. The primary BrC is included with explicit emission inventories scaled to the organic carbon emissions. This assumes BrC as an individual aerosol type emitted separately from other non-absorbing organic aerosol (OA) compounds. Are there observational evidence to support the assumption? It is not clarified if the BrC emissions are then excluded from the total organic aerosol (OA) emissions or not. The double-counting of BrC may lead to artificial increases in OA aerosol mass and total AOD. Similarly, is secondary BrC included as part of the SOA formation or additional SOA formed from aromatics? The rest OA should be non-absorbing, scattering only, and what optical properties are used for the non-absorbing OA? Furthermore, how does this approach differ essentially from Brown et al. (2018)? Both of them parameterize the absorption due to all the OAs (absorbing + non-absorbing) following Sahel et al. (2014). The definition of BrC radiative effect is also a bit confusing. If BrC are emitted separately as an aerosol type with explicit emissions, then the radiative effect of BrC refers to both scattering and absorption.

Author's response: We understand the reviewer's concerns. While BrC is part of OC in the atmosphere, we can treat them separately using different tracers in model simulations. One can treat BrC as a fraction of OC (as in Brown et al., 2018) but assumptions have to be made (for example, the BrC/OC fraction does not change during transport including convective transport, which should change based on aircraft observations (Zhang et al., 2017)). Our simulation approach is more flexible. There is no double counting problem as long as scattering and absorption are treated separately (through different tracers) in the model. We did not account for the scattering effect of BrC such that absorption of BrC can be compared directly to BC. We added a paragraph at the end of section 3.1, lines 188-192: "One important finding by Zhang et al. (2017) is that wet scavenging of BrC during convection differs from BC and OC. Therefore, BrC is simulated using a different tracer from OC in this work unlike Browne et al. (2018). The BrC property of interest is absorption and we assume that the tracer's optical property is light absorption only (no scattering). Consequently, there is no double counting of OC scattering. In the following analysis, the DRE from BrC is for light absorption only such that it can be directly compared to BC."

Second, the main focus of this study is on the BrC heating effect, but it lacks of evaluation of the modeled aerosol absorption. The ratio of BrC absorption to BC is compared with the DC3 and SEAC4RS measurements, however, limited only to the North America. There is no model evaluation of aerosol absorption over the tropics where the BrC heating effect is suggested to be important. It would be useful to know how the modeled aerosol total and spectrally-dependent absorption compare with observations, i.e., AERONET data, with vs without BrC parameterizations. This would provide observational constraints for the

calculated heating effects due to BrC and BC. In addition, Figures 5 shows the comparison of modeled AOD with AERONET and MODIS, but it is unclear if the inclusion of BrC improves the simulated AOD or not?

Author's Response: In general, the effect of aerosol absorption on AERONET AOD is small and this is particularly true for BrC. In Figure 5, we compared AOD from our best model (including BrC absorption) to AERONET and MODIS. The following figure shows modelled AOD without BrC, compared with AERONET and MODIS. It is nearly identical to the results with BrC shown in Figure 5. Quantitively, in fire dominate regions (where BC from fire emissions contributes to >50% of the total BC), BrC contributes ~0.37% of the total AOD and 8.5% of the total absorption aerosol optical depth (AAOD). The increase of AAOD from BrC absorption is more significant than AOD. We added in page 9, lines 274-276, "For these data, the effect of BrC absorption on AOD is small; we estimate that BrC absorption contributes 0.37% of the total AOD and 8.5% of the total absorption aerosol optical depth (AAOD)."

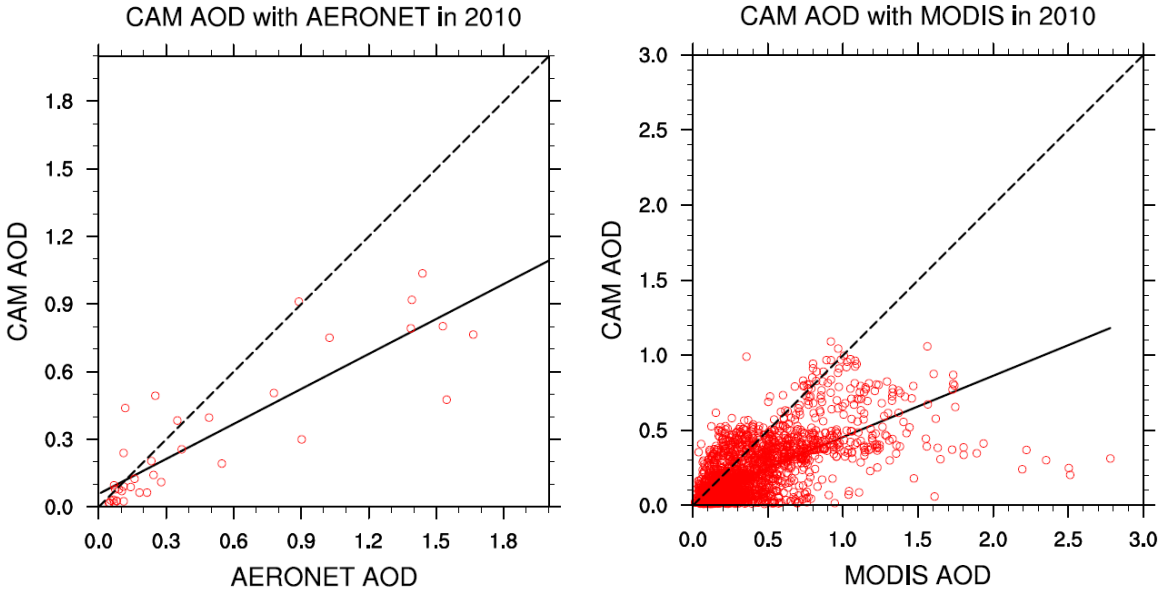

Third, the model sensitivity studies offer limited insights on physical processes. Parameter tuning of the photo-bleaching effects and convective transport of BrC are largely empirical. It is not very convincing, based on Figure 7, to state that the overestimation of BrC/BC ratios in lower troposphere by NCNB (the base mode) and ICNB reflects on the missing of photo-bleaching effect, because it could be due to underestimate of BC. ICB (the best model) that includes the photo-bleaching also overestimates to a similar extent especially when compared with the SEAC4RS data. It is not clear how good or bad these bleaching effects are represented in the model? Or where/when it improves the modeled absorption by BC+BrC? If not, how to improve based on the sensitivity studies conducted? The enhancement of BrC in convective transport is implemented by reducing the wet scavenging efficiency of BrC to match the transported BrC by convective clouds in Zhang et al. (2016). This ignores the impact of uncertainty in model-simulated convective clouds, and possible aqueous formation of secondary BrC in clouds, attributing the BrC changes solely to the scavenging efficiency without justifying it. At least, other factors should be discussed and probably examined in the sensitivity studies.

Author's Response: There are uncertainties in the model simulations. In the conclusion section, lines 461-464, we emphasized the uncertainties: "There are still considerable uncertainties in modeling BrC absorption and its effects in the atmosphere. Parameterizations of emissions, photo-bleaching, and convective transport of BrC all require more field and laboratory observations. The modeling result of stronger heating by BrC than BC over the tropical free troposphere in this study are subject to the

uncertainties. The results from this study indicate that field measurements over tropical convective regions during periods of biomass burning are critically needed to further improve our understanding of BrC processes and its climate effects…"

We added the following figure in the supplement (now Figure S2) to show that that BrC in the NCNB model is much higher than the observations in the lower troposphere. Photo-bleaching, which was observed in field observations, is an obvious reason for the overestimated BrC/BC ratio and BrC concentrations in the lower troposphere in the NCNB model.

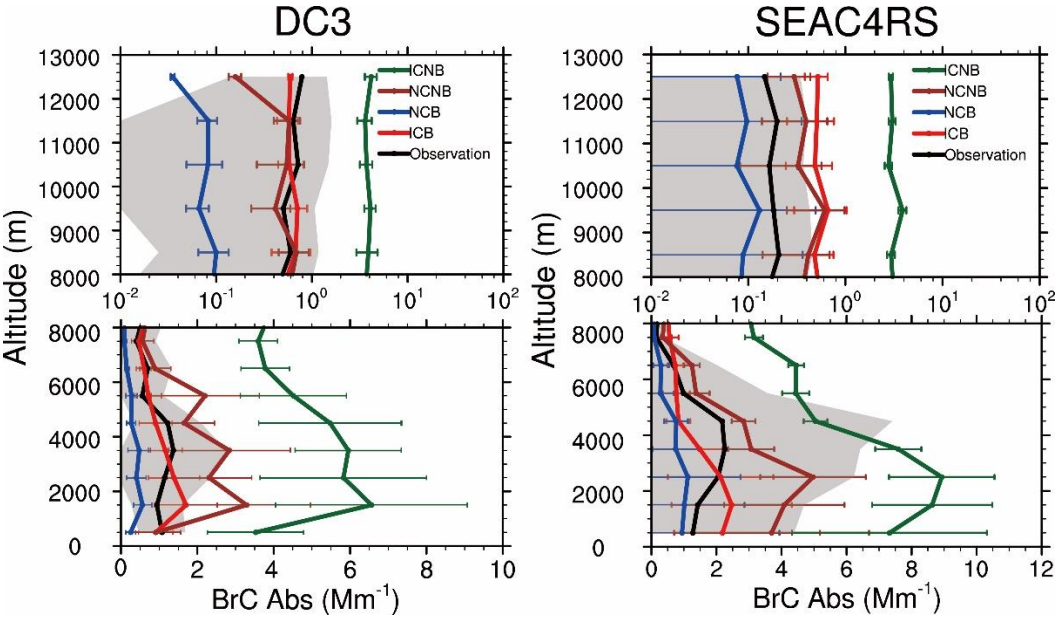

To further address the reviewer's comments, we added a new paragraph at the end of section 5.1, lines 330-337: "In the ICB simulation, wet scavenging of BrC was reduced relative to BC in order to simulate the observed BrC/BC ratios in DC3 and SEAC^{4}RS. The mechanisms are not yet clear due to a lack of laboratory and field observations. Hydrophobic OC, such as humic-like substances (HULIS), is more likely to have high light-absorption compared to hydrophilic OC (Hoffer et al., 2006). BrC with high molecular weight dominates the aged biomass burning plume (Wong et al., 2017, Wong et al., 2019). Since higher molecular weight compounds have lower hygroscopicity (Dinar et al., 2007), and it is harder to activate hydrophobic OC in cloud, less BrC is removed in deep convection. Another possible mechanism is production of BrC through in-cloud heterogeneous processing of fire plumes (Zhang et al., 2017). However, there is no observation data to implement such a mechanism in a model."

Other than the main concerns, a few minor comments are also included:

1. Page 5, line 136: why do you use different reference wavelengths for primary and secondary BrC?

Author's Response: We kept the reference wavelengths from the experiments of McMeeking, (2008) and Nakayama et al. (2010) for primary and secondary BrC. To make MAE references agree with each other, we have converted secondary BrC MAE to 550 nm (0.19 m2/g) using the AAE = 5.0 in the updated manuscript section 3.1, line 144.

2. Page 5, line 137: AAE is highly variable and the estimated BrC absorption is sensitive to AAE. Uncertainty associated with AAE should be discussed and probably examined in sensitivity studies.

Author's Response: Previous modelling study from Jo et al. (2016) estimated BrC/BC absorption ratio with different AAE of BrC. They found BrC/BC ratio will decrease when BrC AAE increase from 5 to 6.19. We used a BrC AAE of 5.0, which also agrees with the experiment results of Kirchstetter and Thatcher (2012). We discussed the uncertainty of BrC simulation coming from AAE variation in the updated manuscript section 3.1, lines 152-156.

3. Page 5, line 139: this equation is confusing. What is the reference? Where is k_OA, from the second step to the third?

Author's Response: The first step from the equation is to convert the imaginary refractive index of OA (BrC + non-absorbing OA) to the imaginary refractive index of BrC. k_{OA} from the second step to the third is based on the Eq.6 in Liu et al., (2013):

$$k = \frac{\rho\lambda \cdot A(\lambda)}{4\pi \cdot c}$$

where k is the imaginary refractive index, ρ is particle density (g m^{-3}), A(λ) is the light absorption at the wavelength λ, and c is the mass concentration.

4. Page 6, line 165: are you using k_OA from Sahel et al., 2014 for OA, after including explicit BrC emissions?

Author's Response: No. We convert k_{OA} to k_{BrC} using Eq.3, and apply it to the Eq.6 in Liu et al. (2013) to get Eq. 5, and we applied k_{BrC} to the explicit BrC emissions. We added after Eq. (4), lines 200-202, "We computed $k_{OA,550}$ in order to calculate BrC emissions. In the model, the absorption of the OC tracer was specified to be 0. All OC absorption was due to the BrC tracer."

5. Page 10, section 5.3, equations (6) and (7): I think that the parameterizations in Sahel et al., (2014) are for absorption spectral dependence of the total OA including both absorbing and non-absorbing components. But here they are applied to the absorbing components only?

Author's Response: Equations (6) and (7) are the functions for the wavelength dependence of imaginary refractive index for all kinds of particles**,** they obey a power relationship with the wavelength ratio and an exponent w. The parameterizations in Saleh et al., (2014), described in Eq. 4, shows a relationship between BC/OA ratio and the k of total OA including both absorbing and non-absorbing components. We convert k_{OA} to k_{BrC} using Eq. 3 and apply it to the absorbing components.

6. Page 10, line 311: please clarify what two sets of radiative fluxes are used to calculate the BrC DRE

Author's Response: We simulated the clear sky net solar flux at the top of atmosphere with all aerosols (FSNTOAC, the BrC tracers have only absorption and no scattering) and the clear sky net solar flux at the top of atmosphere with all aerosols but no BrC absorption (FSNTOAC_noBrC, the BrC tracers have no absorption or scattering). We calculated BrC DRE by subtracting FSNTOAC and FSNTOAC_noBrC. Lines 366-368 is updated with this information.

Brown, H., Liu, X., Feng, Y., Jiang, Y., Wu, M., Lu, Z., Wu, C., Murphy, S. and Pokhrel, R., 2018. Radiative effect and climate impacts of brown carbon with the Community Atmosphere Model (CAM5). Atmospheric Chemistry and Physics, 18, 17745-17768, https://doi.org/10.5194/acp-18-17745-2018, 2018.

Browne, E. C., Zhang, X., Franklin, J. P., Ridley, K. J., Kirchstetter, T. W., Wilson, K. R., Cappa, C. D., and Kroll, J. H.: Effect of heterogeneous oxidative aging on light absorption by biomass-burning organic aerosol, Aerosol Science and Technology, 1-15, https://doi.org/10.1080/02786826.2019.1599321, 2019.

Forrister, H., Liu, J., Scheuer, E., Dibb, J., Ziemba, L., Thornhill, K. L., Anderson, B., Diskin, G., Perring, A. E., and Schwarz, J. P.: Evolution of brown carbon in wildfire plumes, Geophysical Research Letters, 42, 4623-4630, https://doi.org/10.1002/2015GL063897, 2015.

Jo, D. S., Park, R. J., Lee, S., Kim, S.-W., and Zhang, X.: A global simulation of brown carbon: implications for photochemistry and direct radiative effect, Atmospheric Chemistry and Physics, 16, 3413-3432, https://doi.org/10.5194/acp-16-3413-2016, 2016.

Kirchstetter, T., and Thatcher, T.: Contribution of organic carbon to wood smoke particulate matter absorption of solar radiation, Atmospheric Chemistry and Physics, 12, 6067-6072, https://doi.org/10.5194/acp-12-6067-2012, 2012.

Liu, J., Bergin, M., Guo, H., King, L., Kotra, N., Edgerton, E., and Weber, R.: Size-resolved measurements of brown carbon in water and methanol extracts and estimates of their contribution to ambient fine-particle light absorption, Atmospheric Chemistry and Physics, 13, 12389-12404, https://doi.org/10.5194/acp-13-12389-2013, 2013.

McMeeking, G. R.: The optical, chemical, and physical properties of aerosols and gases emitted by the laboratory combustion of wildland fuels, Colorado State University, 2008.

Nakayama, T., Matsumi, Y., Sato, K., Imamura, T., Yamazaki, A., and Uchiyama, A.: Laboratory studies on optical properties of secondary organic aerosols generated during the photooxidation of toluene and the ozonolysis of α-pinene, Journal of Geophysical Research: Atmospheres, 115, https://doi.org/10.1029/2010JD014387, 2010.

Saleh, R., Robinson, E. S., Tkacik, D. S., Ahern, A. T., Liu, S., Aiken, A. C., Sullivan, R. C., Presto, A. A., Dubey, M. K., and Yokelson, R. J.: Brownness of organics in aerosols from biomass burning linked to their black carbon content, Nature Geoscience, 7, 647-650, https://doi.org/10.1038/ngeo2220, 2014.

Wang, X., Heald, C. L., Liu, J., Weber, R. J., Campuzano-Jost, P., Jimenez, J. L., Schwarz, J. P., and Perring, A. E.: Exploring the observational constraints on the simulation of brown carbon, Atmospheric Chemistry and Physics, 18, 635, https://doi.org/10.5194/acp-18-635-2018, 2018.

Zhang, Y., Forrister, H., Liu, J., Dibb, J., Anderson, B., Schwarz, J. P., Perring, A. E., Jimenez, J. L., Campuzano-Jost, P., and Wang, Y.: Top-of-atmosphere radiative forcing affected by brown carbon in the upper troposphere, Nature Geoscience, 10, 486, https://doi.org/10.1038/ngeo2960, 2017.

Modeling global radiative effect of brown carbon: A potentially larger heating source in the tropical free troposphere than black carbon

Aoxing Zhang[1], Yuhang Wang[1], Yuzhong Zhang[1,2], Rodney J Weber[1], Yongjia Song[1], Ziming Ke[1,3], Yufei Zou[1,4]

[1]School of Earth and Atmospheric Sciences, Georgia Institute of Technology, Atlanta, USA
[2]Now at School of Engineering and Applied Sciences, Harvard University, Cambridge, MA, USA
[3]Now at Department of Atmospheric Science, University of Wyoming, Laramie, Wyoming, USA
[4]Now at School of Environmental and Forest Sciences, University of Washington, Seattle, WA, USA

Correspondence to: Yuhang Wang (yuhang.wang@eas.gatech.edu)

Abstract. Carbonaceous aerosols significantly affect global radiative forcing and climate through absorption and scattering of sunlight. Black carbon (BC) and brown carbon (BrC) are light-absorbing carbonaceous aerosols. The direct radiative effect (DRE) of BrC is uncertain. A recent study suggests that BrC absorption is comparable to BC in the upper troposphere over biomass burning regions and that the resulting radiative heating tends to stabilize the atmosphere. Yet current climate models do not include proper physical and chemical treatments of BrC. In this study, we derived a BrC global biomass burning emission inventory on the basis of the Global Fire Emissions Database 4 (GFED4), developed a BrC module in the Community Atmosphere Model version 5 (CAM5) of Community Earth System Model (CESM) model, and investigated the photo-bleaching effect and convective transport of BrC on the basis of Studies of Emissions, Atmospheric Composition, Clouds and Climate Coupling by Regional Surveys (SEAC^{4}RS) and Deep Convective Clouds and Chemistry Project (DC3) measurements. The model simulations of BC were also evaluated using HIAPER (High-Performance Instrumented Airborne Platform for Environmental Research) Pole-to-Pole Observations (HIPPO) measurements. We found that globally BrC is a significant absorber, the DRE of which is 0.10 W/m^2, more than 25% of BC DRE (+0.39 W/m^2). Most significantly, model results indicated that BrC atmospheric heating in the tropical mid and upper troposphere is larger than that of BC. The source of tropical BrC is mainly from wildfires, which are more prevalent in the tropical regions than higher latitudes and release much more BrC relative to BC than industrial sources. While BC atmospheric heating is skewed towards northern mid-latitude lower atmosphere, BrC heating is more centered in the tropical free troposphere. A possible mechanism for the enhanced convective transport of BrC is that hydrophobic high molecular weight BrC becomes a larger fraction of the BrC and less easily activated in a cloud as the aerosol ages. The contribution of BrC heating to the Hadley circulation and latitudinal expansion of the tropics is comparable to BC heating.

1 Introduction

Carbonaceous aerosols, including black carbon (BC) and organic carbon (OC), are important factors in global atmospheric radiative forcing. BC warms the atmosphere by directly absorbing solar radiation (Bond et al., 2013). OC used to be thought to cool the atmosphere due to its light scattering properties. However, some OC, known as "brown carbon" (BrC), absorbs visible light with a wavelength dependence; the efficiency increases rapidly with decreasing wavelength (Hecobian et al., 2010; Kirchstetter and Thatcher, 2012; Kirchstetter et al., 2004; Yang et al., 2009).

The primary source of BrC is incomplete combustion of biomass and biofuel (Chakrabarty et al., 2010; Feng et al., 2013; Desyaterik et al., 2013; Washenfelder et al., 2015). There is evidence that BrC is also associated with fossil fuel combustion and urban emissions (Zhang et al., 2011; Costabile et al., 2017; Yan et al., 2017; Xie et al., 2017). Secondary BrC is mainly produced from the photo-oxidation of volatile organic compounds (VOCs), such as nitrophenols and aromatic carbonyls (Jacobson, 1999; Nakayama et al., 2010; Nakayama et al., 2013), monoterpenes (Laskin et al., 2014), and methylglyoxal (Sareen et al., 2013). Secondary BrC also comes from aqueous-phase reactions in droplets (Updyke et al., 2012; Nguyen et al., 2012) and homogenous and heterogenous reactions of catechol (Pillar et al., 2014; Pillar and Guzman, 2017; Magalhães et al., 2017) and phenolic compounds (Yu et al., 2016; Lavi et al., 2017; Smith et al., 2016). BrC from biomass burning contributes more to light absorption than the other sources (Chakrabarty et al., 2010; Saleh et al., 2014; Kirchstetter and Thatcher, 2012; McMeeking, 2008). Factor analysis of water-soluble organic carbon (WSOC) over the southeastern United States averaged for one year (Hecobian et al., 2010) attributed ~50% of solar absorption at 365 nm to biomass burning emissions, 20-30% to secondary organic carbon, and ~10% to primary urban emissions (mobile sources).

Alexander et al. (2008) analyzed the radiative effects of aerosols in the outflow region of East Asia and found that wood smoke BrC accounted for 14% of total aerosol absorption. Liu et al. (2014) found a ~20% reduction of aerosol cooling from BrC absorption at the top of the atmosphere on the basis of measured BrC vertical profiles. However, current observations do not provide enough constraints on the global BrC radiative forcing (Schuster et al., 2016a; Schuster et al., 2016b).

Global models have been applied to estimate Direct Radiative Forcing (DRF) and Direct Radiative Effects (DRE) of BrC. Aerosol DRE represents the difference of radiative budget with and without aerosols, and DRF represents the difference of DRE between present day and pre-industrial times (Heald et al., 2014). The study by Feng et al. (2013) suggested a +0.04-0.11 W/m^2 warming effect at the top of atmosphere due to the absorption of BrC, and attributed 19% of anthropogenic aerosol absorption to BrC. Wang et al. (2014) estimated the global DRF of +0.11 and +0.21 W/m^2 for BrC and BC, respectively. Jo et al. (2016) estimated a BrC DRE of +0.11 W/m^2. Lin et al. (2014) estimated a BrC DRE of +0.22-0.57 W/m^2, which accounted for 27%-70% of the BC absorption in their model. Park et al. (2010) modeled BrC over East Asia and calculated a DRE of +0.05 W/m^2 at the top of the atmosphere. Brown et al. (2018) estimated a BrC DRE of +0.13±0.01

W/m^2 and 0.01± 0.04 W/m^2 from BrC aerosol-cloud interaction. Saleh et al. (2015) estimated a BrC DRE of 0.22 W/m^2 when BrC externally mixed with BC, and 0.12 W/m^2 when BrC is internally mixed with BC. All of these model estimations of BrC DRE and DRF treated BrC similar to BC, where properties were invariant with atmospheric processing or aging.

~~In this study, we developed and implemented a BrC module in the Community Earth System Model (CESM) to assess the effects of BrC DRE.~~ Laboratory and field studies showed a reduction of BrC absorption when exposed to light, which is usually referred to as "photo-bleaching" (Zhao et al., 2015). A recently global model simulation (Wang et al., 2018) included this effect, constrained with BrC absorption measurements in DC3 and $SEAC^4RS$, resulting in a large reduction of global BrC DRE to +0.048 W/m^2 compared to previous estimates from the studies listed above. Brown~~-~~ et al. (2018) developed a BrC module in the CESM and ~~also~~ showed a reduction of BrC DRE to 0.06±0.008 W/m^2 because of photo-bleaching. Other effects of atmospheric processing have not yet been in BrC global modeling. Results from the Deep Convective Clouds and Chemistry Project (DC3) found high concentrations of BrC in the continental upper tropospheric due to convective transport, suggesting more efficient atmospheric vertical transport of BrC than previously assumed (Zhang et al., 2017). In this study, we developed and implemented a BrC module in the Community Earth System Model (CESM) to assess the effects of BrC DRE. Here, we include these effects and make use of the aircraft measurements of BrC absorption profiles from DC3 and $SEAC^4RS$ campaigns to evaluate the model formulation and simulation results. The global BrC emissions from biomass burning, biofuel emissions, and secondary formation were included. We tested the sensitivity of photo-bleaching effect and the deep convective transport of BrC to its DRE, and estimated the global DRE. Model simulation results without considering the differential convective transport and BC and BrC are compared to previous studies. This is the first attempt to comprehensively analyze how convective transport and photo-bleaching affect global atmospheric heating by BrC absorption relative to BC.

2 Model Description

2.1 The CESM Model

We developed the brown carbon simulation based on the Community Earth System Model (CESM) version 1.2.2 and its atmospheric component, the Community Atmosphere Model version 5 (CAM5) (Neale et al., 2010). The CAM5 model has a comprehensive mechanism for aerosols and cloud-aerosol interaction (Liu et al., 2012; Ghan et al., 2012; Gettelman et al., 2010). The CAM5 radiation scheme is the Rapid Radiative Transfer Method for GCMs (RRTMG), which provides an accurate method for radiative flux calculation (Iacono et al., 2008; Mlawer et al., 1997). The atmospheric chemistry module, turbulence scheme, convection scheme, and cloud physics are coupled in the model (Zhang and McFarlane, 1995; Bretherton and Park, 2009; Park and Bretherton, 2009; Richter and Rasch, 2008; Morrison and Gettelman, 2008). We used a 3-mode version of the modal aerosol model (MAM-3) for aerosol modeling in CAM5. The 3 modes are Aitken, accumulation, and coarse modes (Neale et al., 2010). In our BrC simulations, we used CAM5 with a spatial resolution of 1.9°x2.5°. The wet

scavenging scheme of aerosols in CAM5 includes below-cloud scavenging and in-cloud scavenging, which was found to have a high bias (Wang et al., 2011; Liu et al., 2012). For the simulations used to compare with field observations, we nudged CAM5 meteorological field (temperature, humidity, wind, surface pressure and heat) to GEOS-5.2.0 meteorological data products (Suarez et al., 2008) every 6 hours in order to evaluate the model simulations with BrC observations (Ma et al., 2013; Chipperfield, 2006). We also conducted 5-year free-running model simulations using the climatology of 2010 to analyze the climate response to BrC and BC heating. The spin-up time is 3 months in the nudged CAM5 simulations and is 1 year in the free-running simulations.

2.2 Emissions

We derived global BrC emissions from biomass burning, biofuel, and secondary formation. Same as Brown et al., 2018, we used the parameterization by Saleh et al. (2014) for biomass and biofuel burning, in which emitted BrC absorption is a function of BC/Organic Aerosols (OA) emission ratio. We included secondary aerosols from the oxidation of aromatic as the major source of secondary BrC (Hecobian et al., 2010; Sareen et al., 2013; Lin et al., 2015). Secondary BrC produced from aromatic oxidation absorbs more solar radiation in high-NOx conditions (Laskin et al., 2015; Lin et al., 2015; Liu et al., 2012; Nakayama et al., 2010, 2013; Yu et al., 2014; Zhong and Jang, 2011). We did not consider the NOx dependence of secondary BrC in this study. More details will be described in section 3.

The biomass burning emissions we used are from the Global Fire Emission Database version 4 including small fires (GFED4s) (Giglio et al., 2013; Randerson et al., 2012). It contains global burned area distribution and biomass burning emission factors of related aerosols and gas species for different fire types, with a spatial resolution of 0.25°x0.25°. In CAM5, we aggregated it to a spatial resolution to 1.9°x2.5° and used GFED daily emission and diurnal cycle factors. The different emission factors for tropical forest, temperate forest, boreal forest, savanna, agriculture waste and peat burning are based on Akagi et al. (2011). Fire emissions can reach high altitudes (e.g., Neale et al., 2010). We used an observation-constrained global fire plume rise dataset in which MODIS fire hotspot and fire radiance power data were used in a 1-D fire plume rise model and the resulting fire plume distribution is in good agreement with the Multi-angle Imaging SpectroRadiometer (MISR) observations (Ke, 2019). Biomass burning emissions have high uncertainties caused by burned area, emission factors, fuel loads and combustion completeness factors (Akagi et al., 2011; Giglio et al., 2013), and the complex interactions between fire, terrestrial ecosystem, and climate systems amplify these uncertainties (Zou et al., 2019).

Anthropogenic emissions are from the IPCC AR5 emission dataset (Lamarque et al., 2010), and BC and OC emissions are updated based on the emission inventory of 2000 (Bond et al., 2007; Junker and Liousse, 2008). We increased anthropogenic emissions in China by 50% according to Zhang et al. (2009). For the Arctic region (> 66°N), we used the Evaluating the

Climate and Air Quality Impacts of Short-lived Pollutants (ECLIPSE) emission dataset, which includes an improvement for the Arctic BC emissions (Stohl et al., 2013; Klimont et al., 2015).

For the optical properties of BC, we used 10 and 8.1 m2/g for 345- 442 nm and 442-625 nm, respectively, as the MAE values of BC (Knox et al., 2009; Bond and Bergstrom, 2006). MAM3 assumes that primary carbon is internally mixed with secondary aerosols in the accumulation mode.

3 Brown Carbon Module

3.1 BrC optical property and photo-bleaching

BrC absorption depends on its Mass Absorption Efficiency (MAE), which is the ratio of light absorption in the wavelength λ to BrC mass concentration (m^2 g^{-1}):

$$MAE_{BrC}(\lambda) = \frac{A(\lambda)}{c_{BrC}}. \quad (1)$$

where $A(\lambda)$ represents the absorption of BrC at the wavelength of λ (m^{-1}), and c_{BrC} is the mass concentration of BrC (g m^{-3}).

Similar to Jo et al. (2016), w~~W~~e used a constant MAE value for primary BrC, 1.0 m^2/g at 550 nm (McMeeking, 2008), and we used an MAE value of 0.19 m^2/g at 550 nm for secondary BrC based on the work by Nakayama et al. (2010). There are other MAE estimates in experiments such as 3.6-4.1 m^2/g (Alexander et al., 2008) and 0.58-0.64 m^2/g (Hecobian et al., 2010), and model-specified values such as 0.35 m^2/g by Wang et al. (2018). MAE value may also change in different seasons (Cheng et al., 2011). At present, there are not enough observations to specify variable MAE values in the model. ~~We used an MAE value of 1.5 m^2/g at 365 nm for secondary BrC based on the work by Nakayama et al. (2010).~~ The MAE value at the other wavelengths was calculated using the following function (Bond and Bergstrom, 2006):

$$\mathrm{MAE}(\lambda) = \mathrm{MAE}(\lambda_0) * (\lambda_0/\lambda)^{AAE}, \quad (2)$$

where AAE is absorption Angström exponent, and λ_0 is 550 and 365 nm for primary and secondary BrC, respectively. We used AAE = 5.0 for λ < 2 μm (Jo et al., 2016; Kirchstetter and Thatcher, 2012). BrC AAE varies depending on its source and wavelength used (Kirchstetter and Thatcher, 2012; Liu et al., 2014). Jo et al. (2016) found BrC/BC ratio decreases when the BrC AAE increases from 5 to 6.19, Saleh et al. (2014) also found BC/OA ratio is negatively related to BrC AAE and positively related to BrC absorption. Therefore, the variation of BrC AAE leads to additional uncertainty of the BrC simulation.). ~~In the CESM RRTMG model, T~~the imaginary part of refractive index ~~is 0.0050 in the band of 442 nm to 625 nm for non-absorbing OC. Its value~~ for BrC is estimated using the following equation (Liu et al., 2013):

$$k_{BrC,\lambda} = k_{OA,\lambda} * \frac{c_{OA}}{c_{BrC}} = \frac{\rho\lambda \cdot A(\lambda)}{4\pi \cdot c_{BrC}} = \frac{\rho\lambda \cdot MAE(\lambda)}{4\pi}, \quad (3)$$

where ρ is particle density (g m^{-3}), A(λ) is the light absorption at wavelength λ, and c is mass concentration.

The estimated k_{BrC} value is 0.045 at 550 nm for primary BrC and 0.043 at 365 nm for secondary BrC, respectively.

There is observational evidence that both primary and secondary BrC are affected by photochemical aging (or bleaching), which reduces BrC light absorption when exposed to light (Forrister et al., 2015; Sareen et al., 2013; Lee et al., 2014; Zhong and Jang, 2011; Wong et al., 2017; Wong et al, 2019). Previous modeling of the BrC photo-bleaching effect by Wang et al. (2018) and Brown et al. (2018) applied a 1-day e-folding time for BrC before reaching a threshold of 25% of the original BrC absorption. Our approach to BrC photo-bleaching considers different bleaching effects depending on BrC source. ~~Different components of SOA have different photo-bleaching lifetimes. Aromatic SOA has a half-life of 12-24 hours (Liu et al., 2016; Lee et al., 2014; Zhong and Jang, 2011), limonene SOA has a half-life of <0.5 hours (Lee et al., 2014). Methylglyoxal SOA has a half-life of 90 minutes (Zhao et al., 2015; Wong et al., 2017). Therefore, w~~We specify a decay half-life of 12 hours when light is present for primary biomass and biofuel BrC in the daytime until 6% is left and no further photobleaching occurs (Forrister et al., 2015) due to stable high molecular weight chromophores (Di Lorenzo and Young, 2015; Di Lorenzo et al., 2017; Wong et al., 2017; Wong et al, 2019). Different components of SOA have different photo-bleaching lifetimes. Aromatic SOA has a half-life of 12-24 hours (Liu et al., 2016; Lee et al., 2014; Zhong and Jang, 2011), limonene SOA has a half-life of <0.5 hours (Lee et al., 2014). Methylglyoxal SOA has a half-life of 90 minutes (Zhao et al., 2015; Wong et al., 2017). Therefore, ~~T~~the half-life for secondary aromatic BrC is specified at 12 hours in daytime until it is completely removed (Liu et al., 2016). The other secondary BrCs that have shorter lifetimes contribute little to global radiative forcing and are not included in the model.

The analysis of aircraft BrC observations by Zhang et al. (2017) showed that BrC transported by deep convection plays a significant role in radiative heating of the upper troposphere, and that BrC warming is about one third of BC warming at the tropopause. The standard model simulations show a large low bias of BrC in the upper troposphere compared to the observations by Zhang et al. (2017). In addition, in-cloud heterogeneous BrC production is another possible reason for the high level BrC in the upper troposphere. A fraction of biomass burning BrC from heterogeneous oxidation by ozone will stay free from photo-bleaching, and BrC from heterogeneous oxidations by OH has a long lifetime of days (Browne et al., 2019). Therefore, we conducted sensitivity simulations of BrC to investigate the effects of photo-bleaching and wet scavenging during deep convection.

One important finding by Zhang et al. (2017) is that wet scavenging of BrC during convection differs from BC and OC. Therefore, BrC is simulated using a different tracer from OC in this work unlike Brown et al. (2018). The BrC property of interest is absorption and we assume that the tracer's optical property is light absorption only (no scattering). Consequently, there is no double counting of OC scattering. In the following analysis, the DRE from BrC is for light absorption only such that it can be directly compared to BC.

3.2 BrC Emissions

We assumed that BrC is emitted in the accumulation mode (Liu et al, 2013). Sources of the more stable forms of BrC include primary emissions of biomass burning and biofuel, as well as secondary formation from aromatic oxidation. Similar to previous model approaches (Wang et al., 2018; Brown et al., 2018), b~~B~~iomass burning BrC emissions were parameterized as a function of BC to OA ratio of the emissions (Saleh et al., 2014):

$$k_{OA,550} = 0.016 log_{10}\left(\frac{E_{BC}}{E_{OA}}\right) + 0.03925, \quad (4)$$

where $k_{OA,550}$ is OA absorptivity at 550 nm, and E_{BC} and E_{OA} are BC and OA emission rates (g m^{-2} s^{-1}), respectively. We computed $k_{OA,550}$ in order to calculate BrC emissions. In the model, the absorption of the OC tracer was specified to be 0. All OC absorption was due to the BrC tracer. We scaled BrC Emissions based on $k_{OA,550}$, MAE and OA emissions using the following equation by Liu et al. (2013):

$$E_{BrC} = \frac{4\pi k_{OA,550} \cdot E_{OA}}{\rho \cdot 550nm \cdot MAE_{BrC}(550\ nm)}. \quad (5)$$

where ρ is particle density (g m^{-3}), and E_{BrC} is BrC emission rate (g m^{-2} s^{-1}).

Using the GFED emissions inventory, we estimated an annual average global BrC source from biomass burning of 3.6 TgC/yr, ~23% of OC emissions (15.9 TgC/yr) and about twice as large as BC emissions (1.9 TgC/yr). The variability of BrC emission rate among biomes therefore depends on the BC to OA emission ratios in the GFED emission inventory. Using the same equations and an average E_{BC}/E_{OA} ratio of 0.41 (Junker and Liousse, 2008), we estimated an E_{BrC}/E_{OA} ratio of 0.38 and an annual global BrC biofuel source of 3.1 TgC/yr on the basis of biofuel emission inventory by Bond et al. (2007). The estimates of primary BrC emissions are comparable to previous studies (Table 1). BrC emissions from fossil fuel combustion are not yet well characterized to be included in a global model (Saleh et al., 2014; Xie et al., 2017).

The major fraction of secondary BrC that affects atmospheric heating is formed during the oxidation of aromatics (Jacobson, 1999; Nakayama et al., 2013; Zhong et al., 2012). As in previous studies (Jo et al., 2016; Wang et al., 2014), we assumed that secondary BrC is from aged aromatic SOA. In the CAM5 MAM aerosol mechanism, the SOA mass yield for aromatics oxidation is 15% (Neale et al., 2010; Odum et al., 1997). We estimated a global secondary BrC source of 4.1 TgC/yr in agreement with previous studies.

BrC emissions used in this study and the comparison to previous studies are summarized in Table 1, and the emission distribution is shown in Figure 1. Biofuel emissions are high in China and India, and secondary BrC sources are also large in Europe and North America. Figure 2 shows the annual cycle of BrC emissions in 2010. Biofuel and secondary BrC sources have little seasonal variation in the model, while biomass burning has significant seasonal variation. The BrC source is the highest in August at 18.9 TgC/yr. Biomass burning emission accounts for more than 60% of the BrC emissions in August.

4 Model evaluation

4.1 Black carbon measurements from HIAPER

HIAPER (High-Performance Instrumented Airborne Platform for Environmental Research) Pole-to-Pole Observations (HIPPO) measured atmospheric composition approximately from the Arctic to the Antarctic over the Pacific Ocean (Wofsy, 2011). HIPPO executed 5 missions from January 2009 to September 2011. The flight path of each HIPPO mission is shown in Figure 3. Measurements over continental North America east of 140°W were not included in our model evaluation. BC measurements for particles with a size range of 90-600 nm were made from a single-particle soot photometer (SP2) and we increased measured BC data by a factor of 1.1 to account for larger sized BC in the model evaluation (Schwarz et al., 2010; Schwarz et al., 2013). We make use of HIPPO BC measurements to constrain convective transport and wet scavenging.

Wet scavenging is uncertain in 3-D global modelling of BC (Schwarz et al., 2010; Liu et al., 2011). Wang et al. (2013) tested the sensitivities of different physical mechanisms and found a high sensitivity of BC simulations to convective transport and wet removal. Comparison of CAM5 BC simulations with HIPPO observations in Figure 4 shows large overestimates of BC in the tropics and the upper troposphere. Since the emissions of BC are from the surface, the model high biases in these regions suggest insufficient wet scavenging during convection. Wang et al. (2014) updated the model wet scavenging by scavenging hydrophobic aerosols in convective updrafts and scavenging hydrophilic aerosols from cold clouds. In all simulations of this study, w~~W~~e ~~therefore~~ increased interstitial BC scavenging by a factor of 5 to increase wet scavenging and reduced stratiform liquid-containing cloud based on model evaluations using HIPPO observations.~~decrease simulated BC concentrations in the tropics.~~ The high biases above 300 hPa at mid and high latitudes persisted particularly for HIPPO-1 in January 2009 and HIPPO-2 in November 2009. In winter, the simulated high BC concentrations were above the tropopause level at mid and high latitudes, indicating that convective transport reached too high an altitude. We therefore limited deep convection mass transport to an altitude of 50 hPa below the model estimated tropopause, after which the high biases at mid and high latitudes above 200 hPa were corrected. During HIPPO-3 in March-April 2010, model simulated free tropospheric BC at northern mid and high latitudes were much lower than the observations, suggesting excessive scavenging in the model. We reduced cloud-born BC scavenging to 10% when cloud ice is present and to 50% for the other conditions, which improved the model simulations of free tropospheric BC simulations at mid and high latitudes in HIPPO-3 (and HIPPO-2). The modification slightly worsened the model high bias at northern mid and high latitudes in the summer for HIPPO-5 in August-September 2011 and to a lesser extent for HIPPO-4 in June-July, 2011. Overall, the modified CAM5 model simulates HIPPO BC observations much better than the original version.

4.2 Aerosol optical depth over fire emission dominated regions

Direct assessments of BrC sources using observations are difficult because of limited observations. We can, however, evaluate model simulations of fire aerosols with AOD measurements. For this purpose, we chose the months and regions in

model simulations that >50% of monthly mean AOD data are from fire emissions for 2010. The distribution of model simulated mean AOD for data points selected in this manner are shown in Figure S1(a). For comparison purpose, the ground-based AOD measurements were obtained from the Aerosol Robotic Network (AERONET) (Holben et al., 1998). To compare with model simulated AOD data at 550 nm, the AOD measurements at 500 and 675 nm were used to compute Ångström exponent (Ångström, 1964) and calculate the corresponding AOD values at 550 nm (Kumar et al., 2013). Figure 5(a) compares the monthly mean fire dominated 550 nm AOD observations in 2010 in AERONET with corresponding monthly mean model results for selected months and regions. The correlation coefficient, *r*, is high at 0.88, although the observed AOD data were underestimated implying a low bias in fire emissions.

We also compared AOD with the measurements from Moderate Resolution Imaging Spectroradiometer (MODIS) on Terra (EOS-AM-1) satellite for the months and regions in model simulations that >50% of monthly mean AOD data are from fire emissions for 2010. We used Collection 6 of MODIS level-3 Deep Blue/Dark Target merged product with a resolution of 1°x1° (Platnick et al., 2017). Figure 5(b) shows the comparison. The correlation coefficient, *r*, is lower at 0.67 than the comparison with AERONET observations. One reason is that the high AOD data in the outflow region of the tropical Atlantic from fire emissions over Africa were significantly underestimated (Figure S1(b)); similar low biases were also found in the outflow region of fire emissions in South America. Additionally, CAM5 underestimates AOD at high latitudes (Liu et al., 2012). The general low bias of fire aerosol emissions was also found by Ward et. al. (2012). For these data, the effect of BrC absorption on AOD is small; we estimate that BrC absorption contributes 0.37% of the total AOD and 8.5% of the total absorption aerosol optical depth (AAOD).

5 Results

5.1 Model simulations of BrC for DC3 and SEAC^{4}RS missions

We evaluated BrC model simulations using the measured BrC absorption data from Studies of Emissions, Atmospheric Composition, Clouds and Climate Coupling by Regional Surveys (SEAC^{4}RS) and Deep Convective Clouds and Chemistry Project (DC3) field experiments (Barth et al., 2015; Liu et al., 2013; Zhang et al., 2017). Flight tracks for these experiments were shown in Figure 6. Fresh fire plume data, diagnosed by data points with a correlation coefficient between CO and CH_3CN > 0.5 ~~(De Gouw et al., 2004; Liu et al., 2014)~~, were not included in model evaluation as in previous studies (De Gouw et al., 2004; Liu et al., 2014).

We described in section 3.1 the rationale for sensitivity simulations to evaluate the effects of BrC photo-bleaching and convective wet scavenging. The model sensitivity simulations are listed in Table 2. In the NCNB (base) model, neither effect was included. In the NCB model, the photo-bleaching effect is included. In the ICNB model, the wet scavenging efficiency

of convective transported BrC was decreased from 75% simulated in the base model to 30%, such that ~70% of BrC was transported through convection to the free troposphere as suggested by Zhang et al. (2016). In the ICB model, both photo-bleaching and reduced convective scavenging effects were included. The ICBB model is similar to ICB model, but photo-bleaching of all BrC was included; in the other models including the photo-bleaching effect, only non-convectively transported BrC was affected (Zhang et al., 2017).

Figure 7 shows the observed vertical profiles of BrC absorption to BC ratio (BrC/BC ratio) and concentrations of BC and CO during the DC3 and SEAC^{4}RS experiments in comparison to the corresponding model simulation results. The difference between BC and CO vertical profiles is negligible among the sensitivity simulations. Simulated mean BC concentrations are within the uncertainties of the measurements. The underestimation at 2-5 km during SEAC^{4}RS suggests transport of non-fire BC to this region since the observed enhancement is insignificant for BrC/BC ratio or CO. The higher CO concentrations in the model than the observations, particularly near the surface, suggests that the model overestimates surface CO emissions.

In the observed profile of BrC/BC shown in Figure 7, BrC/BC increases with the altitude. At 12 km, the BrC/BC ratio is ~10 and ~20 times higher than the BrC/BC near the surface during DC3 and SEAC^{4}RS. ~~During DC3 experiment, respectively. Both the observations and model simulations show the increase of BrC/BC ratio at in the upper troposphere.~~ In the sensitivity simulations not including photo-bleaching of BrC (NCNB and ICNB, Table 2), the BrC/BC ratio is higher than the ICB, NCB and ICBB simulations. Non-photo-bleaching simulations overestimate BrC below 5 km in both DC3 and SEAC^{4}RS experiments, reflecting the effect of photo-bleaching. In the NCNB simulation, the BrC/BC ratio is underestimated in the upper troposphere (> 8 km). The comparison between simulations with and without convective transport (ICNB&NCNB and ICB&NCB) indicates that deep convective transport increased upper tropospheric BrC/BC ratio compared to the lower troposphere in better agreement with the observed profiles. When photo-bleaching effect of convectively transported BrC is included in the ICBB simulation, the model cannot reproduce the observed enhancement of BrC/BC ratio in the upper troposphere.

The simulation of NCB, which included efficient convective scavenging and photo-bleaching, clearly underestimated the observed BrC/BC ratios in both DC3 and SEAC^{4}RS, while the simulation of ICNB, which included reduced convective scavenging but no photo-bleaching, significantly overestimated the BrC/BC ratio observations. ~~The overall best model simulation is ICB, which included reduced convective scavenging and photo-bleaching effect for non-convectively transported BrC.~~ During the SEAC^{4}RS experiment, Figures 7 and S2 show that the models overestimated both BC and BrC in the upper troposphere (except NCB, which underestimated BrC in both experiments), and all model simulations except ICNB ~~the BrC/BC in ICB simulation~~ was underestimated the BrC/BC ratio in the upper troposphere and overestimated in the middle-lower troposphere. The simulation bias is mostly due to biases in BC simulation in that BC was overestimated in the upper troposphere and underestimated in the middle-lower troposphere (Figure 7 and Figure S2). It appears that the

model overestimated non-fire BC in the upper troposphere but underestimated non-fire BC in the middle-lower troposphere outside the biomass burning regions. No model simulation captured the increase of the BrC/BC ratio as observed in SEAC4RS. The overall best model simulation is ICB, which included reduced convective scavenging and photo-bleaching effect for non-convectively-transported BrC. Because the ICB simulation is most consistent with the observations among the model simulations, we applied the ICB model simulation to understand the effects of global BrC radiative forcing.

In the ICB simulation, wet scavenging of BrC was reduced relative to BC in order to simulate the observed BrC/BC ratios in DC3 and SEAC^{4}RS. The mechanisms are not yet clear due to a lack of laboratory and field observations. Hydrophobic OC, such as humic-like substances (HULIS), is more likely to have high light-absorption compared to hydrophilic OC (Hoffer et al., 2006). BrC with high molecular weight dominates the aged biomass burning plume (Wong et al., 2017, Wong et al., 2019). Since higher molecular weight compounds have lower hygroscopicity (Dinar et al., 2007), and it is harder to activate hydrophobic OC in cloud, less BrC is removed in deep convection. Another possible mechanism is production of BrC through in-cloud heterogeneous processing of fire plumes (Zhang et al., 2017). However, there is no observation data to implement such a mechanism in a model.

5.2 Simulated global zonal mean distribution of BrC

We performed diagnostic model simulations to investigate the contributions of BrC absorption from biomass burning emissions, biofuel emissions, and secondary formation, respectively. Figure 8 shows the results. Secondary BrC production has a relatively small contribution because of photo-bleaching of secondary BrC is 100%, while a small fraction of BrC is left after photo-bleaching of biomass burning and biofuel BrC (Forrister et al., 2015). Both biofuel and secondary production are largest at northern mid latitudes since they are due to anthropogenic emissions.

Biomass burning BrC shows drastically different distributions from biofuel BrC. The latitudinal maximum is in the tropics and subtropics, with a secondary peak at 60°N due to fires over Canada and Siberia. The vertical extent of biomass burning BrC is much higher than biofuel BrC due to fire plume rise (Ke, 2019) and the higher vertical extent of tropical convection than midlatitudes. While the effect of biofuel BrC is primarily in the lower troposphere, the radiative forcing of biomass burning BrC is much more substantial in the free troposphere and therefore more strongly affects the atmosphere since solar heating of the atmosphere is generally weak.

5.3 Global directive radiative effect of BrC

Aerosol DRE represents the instantaneous radiative effect of aerosols, which is sometimes confused with DRF (Heald et al., 2014, Ghan, 2013). We applied the Rapid Radiative Transfer Method for GCMs (RRTMG) to BrC and BC radiative forcing. We parameterized the imaginary part of BrC refractive index as an external input of RRTMG. As discussed in Section 3.2,

the imaginary refractive index is specified at 0.045 at 550 nm and 0.043 at 365 nm for primary and secondary BrC, respectively. The wavelength boundaries for RRTMG shortwave and longwave are listed in Tables S1a and S1b in the supplement (Neale et al., 2010; Iacono et al., 2008; Mlawer et al., 1997). We calculated the imaginary refractive index at a different wavelength by introducing wavelength dependence *w* (Saleh et al., 2014):

$$w = AAE - 1, \quad (6)$$

$$k_{BrC,\lambda} = k_{BrC,550} \times (\frac{550}{\lambda})^{w}, \quad (7)$$

where $k_{BrC,\lambda}$ denotes the imaginary refractive index of BrC, and *w* is the wave-length dependent AAE value. Calculation and parameterization of MAE and the imaginary refraction index of BrC were discussed in Section 3.1.

In our estimation of BrC DRE, we only considered the absorption of BrC, and the effect of scattering is not considered. We computed the clear sky net solar flux at the top of atmosphere in two simulation, one with BrC tracer absorbing light and the other without. The difference between the two simulations is BrC DRE. The same method was used to calculate BC DRE.

The ICB model calculated global DRE distributions of BrC and BC and the DRE ratio of BrC to BC are shown in Figure 9. For 2010, we estimated the global averaged DRE of BrC absorption at 0.10 W/m^2 in comparison to 0.39 W/m^2 by BC. While the global DRE by BrC is less than BC, regional BrC DRE ~~radiative forcing~~ can be as large as that of BC due to the large difference in emission distributions. BC DRE is large at northern mid latitudes due to anthropogenic emissions from China and India. BrC emissions are relatively low in these regions (Fig. 1) and consequently BC DRE dominates. Over regions with large fire emissions, both BC and BrC are important. Over most regions of the remote tropical ocean, BrC DRE is larger than BC, suggesting broader regional effects by BrC radiative forcing in the tropics. This simulated feature is due to two factors. In the ICB simulation, wet scavenging removes much more BC than BrC. Therefore, BrC is enriched relative to BC in the free troposphere (e.g., Zhang et. al., 2017). In the tropics, the easterly trade wind in the boundary layer become westerlies in the middle and upper troposphere. The regions of boundary layer BC transport and free tropospheric BrC transport are in opposite directions. As a result, the DRE ratio of BrC to BC is low to the east of the fire emission regions and it is high to the west of the fire emission regions.

To discuss our simulation results in the context of previous modeling studies, which did not use the ICB assumptions, we show the annual mean DRE distributions for all model simulations (Table 2) in Figure 10. Comparing the global mean DRE relative change of ICB (0.10 W/m^2) to NCB (0.013 W/m^2) with that of NCNB (0.077 W/m^2) to NCB shows that the global effect of convective scavenging efficiency decrease is larger than photo-bleaching. A similar conclusion can be obtained by comparing the global mean DRE relative change ICNB (0.26 W/m^2) to NCNB with that of ICNB to ICB. The DRE relative change from ICB to ICBB (0.030 W/m^2) indicates the photo-bleaching effect of convectively transported BrC is larger than

the enhancement of BrC convective transport. The 0.013 W/m^2 DRE in the NCB simulation ~~agrees with~~ is lower than previous model studies considering the photo-bleaching effect (Wang et al., 2018; Brown et al., 2018). In the NCB simulation, remote BrC concentrations are mostly affected by the threshold for photo-bleaching, which is 6% in this study (Forrister et al. 2015) in comparison to 25% in Wang et al. (2018) and Brown et al. (2018), causing the difference in the global DRE estimates with photo-bleaching between this work and previous studies. The 0.077 W/m^2 DRE in the NCNB simulation is comparable to previous studies (Feng et al., 2013; Jo et al., 2016; Wang et al., 2014).

Only ICB simulation results are discussed hereafter. Figure 11 shows the seasonally BrC DRE distributions. The seasonal variation is due primarily to biomass burning. Figure 2 shows that the largest fire emissions in August, September, July, and June. While fire emissions are mostly in the tropics in SON, burning at northern mid and high latitudes much more pronounced in JJA in addition to tropical burning.

5.4 Global effects of BrC absorption on the atmosphere

As found by Zhang et al. (2017), the importance of radiative heating by BrC relative to BC increases with altitude due to convective transport. We compared the difference of average vertical profiles of BrC to BC heating rate ratio in Figure 13. Over regions directly affected by convection, where the convective mass flux is >10^{-5} kg/m^2/s, the simulated result is in agreement with Zhang et al. (2017). Globally, the average BrC/BC heating rate ratio is >100% at 400 hPa, indicating in deep convection regions, atmospheric heating of BrC is stronger than that of BC. In comparison, over the regions not directly affected by deep convection, the globally averaged BrC/BC heating rate ratio increases from 9% at surface level to 53% in the upper troposphere. Geographically, Figure 14 shows that the difference between BrC and BC is particularly large over the tropics.

The heating rate from aerosols, especially its vertical profile, has significant implications on cloud dynamics (e.g., Bond et al., 2013), and can also induce feedback from regional circulation and the planetary boundary layer dynamics (e.g., Ramanathan and Carmichael, 2008). We conducted three 5-year free-running model simulations for the present day (the year 2010). In the control simulation, both BrC and BC heat were included. We then conducted sensitivity simulations in which only BrC or BC heating was included. By comparing the sensitivity simulation results to the control simulation, we diagnosed the climate response to differential BrC and BC heating.

The latitudinal and vertical difference between BrC and BC heating (Figures 13 and 14) implies that BrC heating is more dominant in the tropics and tends to decrease the vertical gradient of temperature. Allen et al. (2012) suggested that light-absorbing aerosols may contribute to tropical expansion. They did not consider the effect of BrC, the atmospheric heating effect of which is more concentrated in the tropics than BC heating (Figure 14). Using the latitude where the Mean Meridional Circulation (MMC) at 500 hPa becomes zero on the poleward side of the subtropical maximum to diagnose the

boundary of the tropics (Zhou et al., 2011), we estimated a 1.0° ± 0.9° latitude of tropical expansion due to BrC heating in comparison to a 1.2° ± 2.9° expansion due to BC heating. The large uncertainty comes from 5 years of free-running simulations and the relatively low model spatial resolution. Another effect from BrC heating is the decrease of deep convective mass flux over the upper troposphere (Feingold et al., 2005; Yoshimori and Broccoli, 2008). We estimated a decrease of deep convective mass flux by 4.41×10^{-5} kg/m^2/s or 4.1% over the tropics, which is about one-third of the corresponding BC heating effect (1.52×10^{-4} kg/m^2/s or 12.9%).

Hodnebrog et al. (2016) suggested that biomass burning aerosols suppress precipitation regionally due primarily to aerosol-cloud interactions. On a global basis, BrC heating reduces precipitation by 0.9% ± 7.0%, which is about 60% of the precipitation reduction by BC simulated in the model. Over the tropical region with high-intensity convection and precipitation, BrC heating decreased precipitation by 3.9% ± 17.8%, similarly to that from BC heating (4.0% ± 17.1%). The effect of BrC heating on tropical precipitation (~100%) is larger than on convective mass flux (~1/3) relative to BC heating because of the stronger BrC than BC heating in the upper than lower troposphere (Figures 13 and 14). BrC heating decreased precipitation by 0.3% ± 10.7% in the northern mid and high latitudes, which is much lower than the effect of BC heating (-4.8 ± 13.5%).

6 Conclusions

Light-absorbing aerosols, including BC and BrC, have significant impacts on the global radiative balance. Observational evidence emerged from the DC3 mission of large enhancements of BrC relative to BC over biomass burning regions (Zhang et al., 2017). We developed a module of brown carbon in CESM CAM5 and conducted two sets of model experiments, 2010 with nudged meteorological fields and 5-year free-running simulations. Compared to previous studies which did not consider differential convective transport of BrC and BC, the simulated BrC DREs without (NCNB) and with (NCB) photo-bleaching are comparable to previous studies (Feng et al., 2013; Jo et al., 2016; Wang et al., 2018; Brown et al., 2018). However, e~~E~~valuations with DC3, SEAC^{4}RS, and HIPPO observations suggested that the model could simulate the observed concentrations of BrC and BC, although model biases were also found. Reducing the convective scavenging efficiency and including photo-bleaching were necessary to simulate the observed BrC distributions. Globally, the former effect is larger than the latter on simulated BrC absorption. Since the two factors have opposite effects on simulated BrC DRE, our best estimation of global DRE of BrC is 0.10 W/m^2~~, which is comparable to previous studies (Feng et al., 2013; Jo et al., 2016)~~.

The BrC DRE is estimated to be 25% of that of BC. Since biomass burning emissions tend to occur during the warm seasons when solar insolation is strong and these emissions tend to occur in the tropics when convective transport is active, the proportional contribution to BrC DRE by biomass burning emission is larger than its fraction in the total emissions. For example, biofuel BrC emissions are seasonal and occur in mid and high latitudes, the combination of BrC absorption and

solar radiation of biofuel BrC is less than biomass burning BrC for a unit of BrC emission. Relative to BC DRE, BrC DRE tends to be larger in the tropics due to different emission distributions and larger BrC levels in the upper troposphere. BrC heating reduces global precipitation by 0.9%, about 60% of the BC induced precipitation decrease. Over the tropics, the reduction of precipitation due to BrC heating is similar to BC heating, but its effect on reducing tropical convective mass flux is only ~1/3 of BC heating because BrC heating is strongly skewed to high altitudes compared to BC heating. Consequently, the effect of BrC heating on tropical expansion is comparable to BC heating.

There are still considerable uncertainties in modeling BrC absorption and its effects in the atmosphere. Parameterizations of e~~-E~~missions, photo-bleaching, and convective transport of BrC all require more field and laboratory observations. The modeling result of stronger atmospheric heating by BrC than BC over the tropical free troposphere in this study are subject to these uncertainties. ~~The results from this study indicate that F~~field measurements over tropical convective regions during periods of biomass burning are critically needed to further improve our understanding of BrC processes and its climate effects. Continuous model development by coupling BrC related processes and climate effects into an interactive climate-fire-ecosystem model (Zou et al., 2019) in CESM would also benefit future projections of climate radiative forcing given large impacts of fire emitted BrC in the tropics found by this study.

Data availability. NASA DC3 and SEAC^{4}RS missions and are available to the general public through the NASA data archive (https://www-air.larc.nasa.gov/cgi-bin/ArcView/dc3 and https://www-air.larc.nasa.gov/cgi-bin/ArcView/seac4rs). MODIS Terra level 3 monthly dataset (MOD08_M3) is available via NASA LAADS Archive (https://ladsweb.modaps.eosdis.nasa.gov/archive/allData/61/MOD08_M3/). HIPPO merged 10-second data is available via CDIAC HIPPO data archive (https://hippo.ornl.gov/data_access). AERONET AOD measurements are available in https://aeronet.gsfc.nasa.gov/new_web/download_all_v3_aod.html. The CAM5 model results are available from the corresponding author upon request.

Competing interests. The authors declare that they have no conflict of interest.

Author contribution. Yuzhong Zhang and Rodney Weber provided the original idea. Aoxing Zhang, Yuhang Wang and Yufei Zou designed the model experiments. Yongjia Song and Ziming Ke conducted and provided the model input data. Rodney Weber and Yuzhong Zhang conducted and analyzed aircraft measurement data. Aoxing Zhang carried out the model experiments and prepared the manuscript with contributions from all co-authors.

Acknowledgments. This work was supported by the National Science Foundation (NSF) through grant 1243220. we would like to acknowledge high-performance computing support from Cheyenne (Computational and Information Systems Laboratory, 2017) and Yellowstone (ark:/85065/d7w3xhc) provided by National Center for Atmospheric Research

(NCAR)'s Computational & Information Systems Lab (CISL), sponsored by the National Science Foundation. We thank Haviland Forrister for helpful discussion.

References

Akagi, S., Yokelson, R. J., Wiedinmyer, C., Alvarado, M., Reid, J., Karl, T., Crounse, J., and Wennberg, P.: Emission factors for open and domestic biomass burning for use in atmospheric models, Atmospheric Chemistry and Physics, 11, 4039-4072, https://doi.org/10.5194/acp-11-4039-2011, 2011.

Alexander, D. T., Crozier, P. A., and Anderson, J. R.: Brown carbon spheres in East Asian outflow and their optical properties, Science, 321, 833-836, https://doi.org/ 10.1126/science.1155296, 2008

Allen, R. J., Sherwood, S. C., Norris, J. R., and Zender, C. S.: Recent Northern Hemisphere tropical expansion primarily driven by black carbon and tropospheric ozone, Nature, 485, 350-354, https://doi.org/10.1038/nature11097, 2012

Ångström, A.: The parameters of atmospheric turbidity, Tellus, 16, 64-75, 1964.

Barth, M. C., Cantrell, C. A., Brune, W. H., Rutledge, S. A., Crawford, J. H., Huntrieser, H., Carey, L. D., MacGorman, D., Weisman, M., Pickering, K. E. and Bruning, E.: The deep convective clouds and chemistry (DC3) field campaign. Bulletin of the American Meteorological Society, 96(8), 1281-1309, https://doi.org/10.1175/BAMS-D-13-00290.1, 2015.

Bond, T. C., and Bergstrom, R. W.: Light absorption by carbonaceous particles: An investigative review, Aerosol science and technology, 40, 27-67, https://doi.org/10.1080/02786820500421521, 2006

Bond, T. C., Bhardwaj, E., Dong, R., Jogani, R., Jung, S., Roden, C., Streets, D. G., and Trautmann, N. M.: Historical emissions of black and organic carbon aerosol from energy-related combustion, 1850–2000, Global Biogeochemical Cycles, 21, https://doi.org/10.1029/2006GB002840, 2007.

Bond, T. C., Doherty, S. J., Fahey, D., Forster, P., Berntsen, T., DeAngelo, B., Flanner, M., Ghan, S., Kärcher, B., and Koch, D.: Bounding the role of black carbon in the climate system: A scientific assessment, Journal of Geophysical Research: Atmospheres, 118, 5380-5552, https://doi.org/10.1002/jgrd.50171, 2013.

Bretherton, C. S., and Park, S.: A new moist turbulence parameterization in the Community Atmosphere Model, Journal of Climate, 22, 3422-3448, https://doi.org/10.1175/2008JCLI2556.1, 2009.

Brown, H., Liu, X., Feng, Y., Jiang, Y., Wu, M., Lu, Z., Wu, C., Murphy, S. and Pokhrel, R., 2018. Radiative effect and climate impacts of brown carbon with the Community Atmosphere Model (CAM5). Atmospheric Chemistry and Physics, 18, 17745-17768, https://doi.org/10.5194/acp-18-17745-2018, 2018.

Browne, E. C., Zhang, X., Franklin, J. P., Ridley, K. J., Kirchstetter, T. W., Wilson, K. R., Cappa, C. D., and Kroll, J. H.: Effect of heterogeneous oxidative aging on light absorption by biomass-burning organic aerosol, Aerosol Science and Technology, 1-15, https://doi.org/10.1080/02786826.2019.1599321, 2019.

Chakrabarty, R., Moosmüller, H., Chen, L.-W., Lewis, K., Arnott, W., Mazzoleni, C., Dubey, M., Wold, C., Hao, W., and Kreidenweis, S.: Brown carbon in tar balls from smoldering biomass combustion, Atmospheric Chemistry and Physics, 10, 6363-6370, https://doi.org/ 10.5194/acp-10-6363-2010, 2010.

Cheng, Y., He, K.-B., Zheng, M., Duan, F.-K., Du, Z.-Y., Ma, Y.-L., Tan, J.-H., Yang, F.-M., Liu, J.-M., and Zhang, X.-L.: Mass absorption efficiency of elemental carbon and water-soluble organic carbon in Beijing, China, Atmospheric Chemistry and Physics, 11, 11497-11510, https://doi.org/10.5194/acp-11-11497-2011, 2011.

Chipperfield, M.: New version of the TOMCAT/SLIMCAT off-line chemical transport model: Intercomparison of stratospheric tracer experiments, Quarterly Journal of the Royal Meteorological Society, 132, 1179-1203, https://doi.org/10.1256/qj.05.51, 2006.

Computational and Information Systems Laboratory: Cheyenne: HPE/SGI ICE XA System (University Community Computing). Boulder, CO: National Center for Atmospheric Research. https://doi.org/10.5065/D6RX99HX, 2017

Costabile, F., Gilardoni, S., Barnaba, F., Ianni, A. D., Liberto, L. D., Dionisi, D., Manigrasso, M., Paglione, M., Poluzzi, V., and Rinaldi, M.: Characteristics of brown carbon in the urban Po Valley atmosphere, Atmospheric Chemistry and Physics, 17, 313-326, https://doi.org/10.5194/acp-17-313-2017, 2017.

Dinar, E., Taraniuk, I., Graber, E.R., Anttila, T., Mentel, T.F. and Rudich, Y.: Hygroscopic growth of atmospheric and model humic-like substances. Journal of Geophysical Research: Atmospheres, 112(D5), https://doi.org/10.1029/2006JD007442, 2007.

De Gouw, J., Cooper, O., Warneke, C., Hudson, P., Fehsenfeld, F., Holloway, J., Hübler, G., Nicks Jr, D., Nowak, J., and Parrish, D.: Chemical composition of air masses transported from Asia to the US West Coast during ITCT 2K2: Fossil fuel combustion versus biomass-burning signatures, Journal of Geophysical Research: Atmospheres, 109, https://doi.org/10.1029/2003JD004202, 2004.

Desyaterik, Y., Sun, Y., Shen, X., Lee, T., Wang, X., Wang, T., and Collett, J. L.: Speciation of "brown" carbon in cloud water impacted by agricultural biomass burning in eastern China, Journal of Geophysical Research: Atmospheres, 118, 7389-7399, https://doi.org/10.1002/jgrd.50561, 2013.

Di Lorenzo, R. A., and Young C. J.: Size separation method for absorption characterization in brown carbon: Application to an aged biomass burning sample, Geophys. Res. Lett., 43, 458-465, https://doi.org/10.1002/2015GL066954, 2015.

Di Lorenzo, R. A., Washenfelder R. A., Attwood, A. R., Guo, H., Xu, L., Ng, S., Weber, R. J., Baumann, K., Edgerton, E., and Young, C. J.: Molecular-Size-Separated Brown Carbon Absorption for Biomass-Burning Aerosol at Multiple Field Sites, Envir. Sci. Technol, 51, 3128-3137, 2017.Feingold, G., Jiang, H., and Harrington, J. Y.: On smoke suppression of clouds in Amazonia, Geophysical Research Letters, 32, https://doi.org/10.1029/2004GL021369, 2005.

Feng, Y., Ramanathan, V., and Kotamarthi, V. R.: Brown carbon: a significant atmospheric absorber of solar radiation?, Atmospheric Chemistry and Physics, 13, 8607-8621, https://doi.org/10.5194/acp-13-8607-2013, 2013.

Fernandes, S. D., Trautmann, N. M., Streets, D. G., Roden, C. A., and Bond, T. C.: Global biofuel use, 1850–2000, Global Biogeochemical Cycles, 21, https://doi.org/10.1029/2006GB002836, 2007.

Forrister, H., Liu, J., Scheuer, E., Dibb, J., Ziemba, L., Thornhill, K. L., Anderson, B., Diskin, G., Perring, A. E., and Schwarz, J. P.: Evolution of brown carbon in wildfire plumes, Geophysical Research Letters, 42, 4623-4630, https://doi.org/10.1002/2015GL063897, 2015.

Gettelman, A., Liu, X., Ghan, S. J., Morrison, H., Park, S., Conley, A., Klein, S. A., Boyle, J., Mitchell, D., and Li, J. L.: Global simulations of ice nucleation and ice supersaturation with an improved cloud scheme in the Community Atmosphere Model, Journal of Geophysical Research: Atmospheres, 115, https://doi.org/10.1029/2009JD013797, 2010.

Ghan, S. J., Liu, X., Easter, R. C., Zaveri, R., Rasch, P. J., Yoon, J.-H., and Eaton, B.: Toward a minimal representation of aerosols in climate models: Comparative decomposition of aerosol direct, semidirect, and indirect radiative forcing, Journal of Climate, 25, 6461-6476, https://doi.org/10.1175/JCLI-D-11-00650.1, 2012.

Ghan, S. J.: Technical Note: Estimating aerosol effects on cloud radiative forcing, Atmospheric Chemistry and Physics, 13, 9971-9974, https://doi.org/10.5194/acp-13-9971-2013, 2013.

Giglio, L., Randerson, J. T., and Werf, G. R.: Analysis of daily, monthly, and annual burned area using the fourth-generation global fire emissions database (GFED4), Journal of Geophysical Research: Biogeosciences, 118, 317-328, https://doi.org/10.1002/jgrg.20042, 2013.

Heald, C.L., Ridley, D.A., Kroll, J.H., Barrett, S.R.H., Cady-Pereira, K.E., Alvarado, M.J. and Holmes, C.D.: Contrasting the direct radiative effect and direct radiative forcing of aerosols. Atmospheric Chemistry and Physics, 14, 5513-5527, https://doi.org/10.5194/acp-14-5513-2014, 2013.

Hecobian, A., Zhang, X., Zheng, M., Frank, N., Edgerton, E. S., and Weber, R. J.: Water-Soluble Organic Aerosol material and the light-absorption characteristics of aqueous extracts measured over the Southeastern United States, Atmospheric Chemistry and Physics, 10, 5965-5977, https://doi.org/10.5194/acp-10-5965-2010, 2010.

Hodnebrog, Ø., Myhre, G., Forster, P. M., Sillmann, J., and Samset, B. H.: Local biomass burning is a dominant cause of the observed precipitation reduction in southern Africa, Nature communications, 7, https://doi.org/10.1038/ncomms11236, 2016.

Hoffer, A., Gelencsér, A., Guyon, P., Kiss, G., Schmid, O., Frank, G.P., Artaxo, P. and Andreae, M.O.: Optical properties of humic-like substances (HULIS) in biomass-burning aerosols, Atmospheric Chemistry and Physics, 6(11), 3563-3570, https://doi.org/10.5194/acp-6-3563-2006, 2006.

Holben, B. N., Eck, T., Slutsker, I., Tanre, D., Buis, J., Setzer, A., Vermote, E., Reagan, J., Kaufman, Y., and Nakajima, T.: AERONET—A federated instrument network and data archive for aerosol characterization, Remote sensing of environment, 66, 1-16, https://doi.org/10.1016/S0034-4257(98)00031-5, 1998.

Iacono, M. J., Delamere, J. S., Mlawer, E. J., Shephard, M. W., Clough, S. A., and Collins, W. D.: Radiative forcing by long-lived greenhouse gases: Calculations with the AER radiative transfer models, Journal of Geophysical Research: Atmospheres, 113, https://doi.org/10.1029/2008JD009944, 2008.

Jacobson, M. Z.: Isolating nitrated and aromatic aerosols and nitrated aromatic gases as sources of ultraviolet light absorption, Journal of Geophysical Research: Atmospheres, 104, 3527-3542, https://doi.org/10.1029/1998JD100054, 1999.

Jo, D. S., Park, R. J., Lee, S., Kim, S.-W., and Zhang, X.: A global simulation of brown carbon: implications for photochemistry and direct radiative effect, Atmospheric Chemistry and Physics, 16, 3413-3432, https://doi.org/10.5194/acp-16-3413-2016, 2016.

Junker, C., and Liousse, C.: A global emission inventory of carbonaceous aerosol from historic records of fossil fuel and biofuel consumption for the period 1860–1997, Atmospheric Chemistry and Physics, 8, 1195-1207, https://doi.org/10.5194/acp-8-1195-2008, 2008.

Ke, Z.: The Global Plume-rise Dataset and Its Climate Model Implement, in preparation, 2019.

Kirchstetter, T., and Thatcher, T.: Contribution of organic carbon to wood smoke particulate matter absorption of solar radiation, Atmospheric Chemistry and Physics, 12, 6067-6072, https://doi.org/10.5194/acp-12-6067-2012, 2012.

Kirchstetter, T. W., Novakov, T., and Hobbs, P. V.: Evidence that the spectral dependence of light absorption by aerosols is affected by organic carbon, Journal of Geophysical Research: Atmospheres, 109, https://doi.org/10.1029/2004JD004999, 2004.

Kumar, K. R., Sivakumar, V., Reddy, R., Gopal, K. R., and Adesina, A. J.: Inferring wavelength dependence of AOD and Ångström exponent over a sub-tropical station in South Africa using AERONET data: Influence of meteorology, long-range transport and curvature effect, Science of the Total Environment, 461, 397-408, https://doi.org/10.1016/j.scitotenv.2013.04.095, 2013.

Lamarque, J.-F., Bond, T. C., Eyring, V., Granier, C., Heil, A., Klimont, Z., Lee, D., Liousse, C., Mieville, A., and Owen, B.: Historical (1850–2000) gridded anthropogenic and biomass burning emissions of reactive gases and aerosols: methodology and application, Atmospheric Chemistry and Physics, 10, 7017-7039, https://doi.org/10.5194/acp-10-7017-2010, 2010.

Lambe, A. T., Cappa, C. D., Massoli, P., Onasch, T. B., Forestieri, S. D., Martin, A. T., Cummings, M. J., Croasdale, D. R., Brune, W. H., and Worsnop, D. R.: Relationship between oxidation level and optical properties of secondary organic aerosol, Environmental science & technology, 47, 6349-6357, https://doi.org/10.1021/es401043j, 2013.

Laskin, A., Laskin, J., and Nizkorodov, S. A.: Chemistry of atmospheric brown carbon, Chemical reviews, 115, 4335-4382, https://doi.org/10.1021/cr5006167, 2015.

Laskin, J., Laskin, A., Nizkorodov, S. A., Roach, P., Eckert, P., Gilles, M. K., Wang, B., Lee, H. J., and Hu, Q.: Molecular selectivity of brown carbon chromophores, Environmental science & technology, 48, 12047-12055, https://doi.org/10.1021/es503432r, 2014.

Lavi, A., Lin, P., Bhaduri, B., Carmieli, R., Laskin, A., and Rudich, Y.: Characterization of light-absorbing oligomers from reactions of phenolic compounds and Fe (III), ACS Earth and Space Chemistry, 1, 637-646, https://doi.org/10.1021/acsearthspacechem.7b00099, 2017.

Lee, H. J., Aiona, P. K., Laskin, A., Laskin, J., and Nizkorodov, S. A.: Effect of solar radiation on the optical properties and molecular composition of laboratory proxies of atmospheric brown carbon, Environmental science & technology, 48, 10217-10226, https://doi.org/10.1021/es502515r, 2014.

Lin, G., Penner, J. E., Flanner, M. G., Sillman, S., Xu, L., and Zhou, C.: Radiative forcing of organic aerosol in the atmosphere and on snow: Effects of SOA and brown carbon, Journal of Geophysical Research: Atmospheres, 119, 7453-7476, https://doi.org/10.1002/2013JD021186, 2014.

Lin, P., Liu, J., Shilling, J. E., Kathmann, S. M., Laskin, J., and Laskin, A.: Molecular characterization of brown carbon (BrC) chromophores in secondary organic aerosol generated from photo-oxidation of toluene, Physical Chemistry Chemical Physics, 17, 23312-23325, https://doi.org/10.1039/C5CP02563J, 2015.

Liu, J., Fan, S., Horowitz, L. W., and Levy, H.: Evaluation of factors controlling long-range transport of black carbon to the Arctic, Journal of Geophysical Research: Atmospheres, 116, https://doi.org/10.1029/2010JD015145, 2011.

Liu, J., Bergin, M., Guo, H., King, L., Kotra, N., Edgerton, E., and Weber, R.: Size-resolved measurements of brown carbon in water and methanol extracts and estimates of their contribution to ambient fine-particle light absorption, Atmospheric Chemistry and Physics, 13, 12389-12404, https://doi.org/10.5194/acp-13-12389-2013, 2013.

Liu, J., Scheuer, E., Dibb, J., Ziemba, L. D., Thornhill, K., Anderson, B. E., Wisthaler, A., Mikoviny, T., Devi, J. J., and Bergin, M.: Brown carbon in the continental troposphere, Geophysical Research Letters, 41, 2191-2195, https://doi.org/10.1002/2013GL058976, 2014.

Liu, J., Lin, P., Laskin, A., Laskin, J., Kathmann, S. M., Wise, M., Caylor, R., Imholt, F., Selimovic, V., and Shilling, J. E.: Optical properties and aging of light-absorbing secondary organic aerosol, Atmospheric Chemistry and Physics, 16, 12815-12827, https://doi.org/10.5194/acp-16-12815-2016, 2016.

Liu, X., Easter, R. C., Ghan, S. J., Zaveri, R., Rasch, P., Shi, X., Lamarque, J.-F., Gettelman, A., Morrison, H., and Vitt, F.: Toward a minimal representation of aerosols in climate models: Description and evaluation in the Community Atmosphere Model CAM5, Geoscientific Model Development, 5, 709, https://doi.org/10.5194/gmd-5-709-2012, 2012.

Ma, P. L., Rasch, P. J., Wang, H., Zhang, K., Easter, R. C., Tilmes, S., Fast, J. D., Liu, X., Yoon, J. H., and Lamarque, J. F.: The role of circulation features on black carbon transport into the Arctic in the Community Atmosphere Model version 5 (CAM5), Journal of Geophysical Research: Atmospheres, 118, 4657-4669, https://doi.org/10.1002/jgrd.50411, 2013.

Magalhães, A. C. O., Esteves da Silva, J. C., and Pinto da Silva, L. s.: Density functional theory calculation of the absorption properties of brown carbon chromophores generated by catechol heterogeneous ozonolysis, ACS Earth and Space Chemistry, 1, 353-360, https://doi.org/10.1021/acsearthspacechem.7b00061, 2017.

McMeeking, G. R.: The optical, chemical, and physical properties of aerosols and gases emitted by the laboratory combustion of wildland fuels, Colorado State University, 2008.

Mlawer, E. J., Taubman, S. J., Brown, P. D., Iacono, M. J., and Clough, S. A.: Radiative transfer for inhomogeneous atmospheres: RRTM, a validated correlated-k model for the longwave, Journal of Geophysical Research: Atmospheres, 102, 16663-16682, http://doi.org/10.1029/97JD00237, 1997.

Morrison, H., and Gettelman, A.: A new two-moment bulk stratiform cloud microphysics scheme in the Community Atmosphere Model, version 3 (CAM3). Part I: Description and numerical tests, Journal of Climate, 21, 3642-3659, https://doi.org/10.1175/2008JCLI2105.1, 2008.

Nakayama, T., Matsumi, Y., Sato, K., Imamura, T., Yamazaki, A., and Uchiyama, A.: Laboratory studies on optical properties of secondary organic aerosols generated during the photooxidation of toluene and the ozonolysis of α-pinene, Journal of Geophysical Research: Atmospheres, 115, https://doi.org/10.1029/2010JD014387, 2010.

Nakayama, T., Sato, K., Matsumi, Y., Imamura, T., Yamazaki, A., and Uchiyama, A.: Wavelength and NO x dependent complex refractive index of SOAs generated from the photooxidation of toluene, Atmospheric Chemistry and Physics, 13, 531-545, https://doi.org/10.5194/acp-13-531-2013, 2013.

Neale, R. B., Chen, C.-C., Gettelman, A., Lauritzen, P. H., Park, S., Williamson, D. L., Conley, A. J., Garcia, R., Kinnison, D., and Lamarque, J.-F.: Description of the NCAR community atmosphere model (CAM 5.0), NCAR Tech. Note NCAR/TN-486+ STR, 2010.

Nguyen, T. B., Lee, P. B., Updyke, K. M., Bones, D. L., Laskin, J., Laskin, A., and Nizkorodov, S. A.: Formation of nitrogen-and sulfur-containing light-absorbing compounds accelerated by evaporation of water from secondary organic aerosols, Journal of Geophysical Research: Atmospheres, 117, http://doi.org/10.1029/2011JD016944, 2012.

Odum, J. R., Jungkamp, T., Griffin, R. J., Forstner, H., Flagan, R. C., and Seinfeld, J. H.: Aromatics, reformulated gasoline, and atmospheric organic aerosol formation, Environmental Science & Technology, 31, 1890-1897, https://doi.org/10.1021/es960535l, 1997.

Park, R. J., Kim, M. J., Jeong, J. I., Youn, D., and Kim, S.: A contribution of brown carbon aerosol to the aerosol light absorption and its radiative forcing in East Asia, Atmospheric environment, 44, 1414-1421, https://doi.org/10.1016/j.atmosenv.2010.01.042, 2010.

Park, S., and Bretherton, C. S.: The University of Washington shallow convection and moist turbulence schemes and their impact on climate simulations with the Community Atmosphere Model, Journal of Climate, 22, 3449-3469, https://doi.org/10.1175/2008JCLI2557.1, 2009.

Pillar, E. A., Camm, R. C., and Guzman, M. I.: Catechol oxidation by ozone and hydroxyl radicals at the air–water interface, Environmental science & technology, 48, 14352-14360, https://doi.org/10.1021/es504094x, 2014.

Pillar, E. A., and Guzman, M. I.: Oxidation of substituted catechols at the air–water interface: Production of carboxylic acids, quinones, and polyphenols, Environmental science & technology, 51, 4951-4959, https://doi.org/10.1021/acs.est.7b00232, 2017.

Platnick, S., et al.: MODIS Atmosphere L3 Monthly Product. NASA MODIS Adaptive Processing System, Goddard Space Flight Center, USA, http://dx.doi.org/10.5067/MODIS/MOD08_M3.061, 2017

Ramanathan, V., and Carmichael, G.: Global and regional climate changes due to black carbon, Nature geoscience, 1, 221-227, https://doi.org/10.1038/ngeo156, 2008.

Randerson, J., Chen, Y., Werf, G., Rogers, B., and Morton, D.: Global burned area and biomass burning emissions from small fires, Journal of Geophysical Research: Biogeosciences, 117, https://doi.org/10.1029/2012JG002128, 2012.

Richter, J. H., and Rasch, P. J.: Effects of convective momentum transport on the atmospheric circulation in the Community Atmosphere Model, version 3, Journal of Climate, 21, 1487-1499, https://doi.org/10.1175/2007JCLI1789.1, 2008.

Saleh, R., Robinson, E. S., Tkacik, D. S., Ahern, A. T., Liu, S., Aiken, A. C., Sullivan, R. C., Presto, A. A., Dubey, M. K., and Yokelson, R. J.: Brownness of organics in aerosols from biomass burning linked to their black carbon content, Nature Geoscience, 7, 647-650, https://doi.org/10.1038/ngeo2220, 2014.

Saleh, R., Marks, M., Heo, J., Adams, P. J., Donahue, N. M., & Robinson, A. L.: Contribution of brown carbon and lensing to the direct radiative effect of carbonaceous aerosols from biomass and biofuel burning emissions. Journal of Geophysical Research: Atmospheres, 120(19), https://doi.org/10.1002/ 2015JD023697, 2015.

Sareen, N., Moussa, S. G., and McNeill, V. F.: Photochemical aging of light-absorbing secondary organic aerosol material, The Journal of Physical Chemistry A, 117, 2987-2996, https://doi.org/10.1021/jp309413j, 2013.

Schuster, G., Dubovik, O., and Arola, A.: Remote sensing of soot carbon–Part 1: Distinguishing different absorbing aerosol species, Atmospheric Chemistry and Physics, 16, 1565-1585, https://doi.org/10.5194/acp-16-1565-2016, 2016a.

Schuster, G., Dubovik, O., Arola, A., Eck, T., and Holben, B.: Remote sensing of soot carbon–Part 2: Understanding the absorption Ångström exponent, Atmospheric Chemistry and Physics, 16, 1587-1602, https://doi.org/10.5194/acp-16-1587-2016, 2016b.

Schwarz, J., Spackman, J., Gao, R., Watts, L., Stier, P., Schulz, M., Davis, S., Wofsy, S., and Fahey, D.: Global-scale black carbon profiles observed in the remote atmosphere and compared to models, Geophysical Research Letters, 37, https://doi.org/10.1029/2010GL044372, 2010.

Schwarz, J., Samset, B., Perring, A., Spackman, J., Gao, R., Stier, P., Schulz, M., Moore, F., Ray, E. A., and Fahey, D.: Global-scale seasonally resolved black carbon vertical profiles over the Pacific, Geophysical research letters, 40, 5542-5547, https://doi.org/10.1002/2013GL057775, 2013.

Smith, J. D., Kinney, H., and Anastasio, C.: Phenolic carbonyls undergo rapid aqueous photodegradation to form low-volatility, light-absorbing products, Atmospheric environment, 126, 36-44, https://doi.org/10.1016/j.atmosenv.2015.11.035, 2016.

Stohl, A., Klimont, Z., Eckhardt, S., Kupiainen, K., Shevchenko, V. P., Kopeikin, V., and Novigatsky, A.: Black carbon in the Arctic: the underestimated role of gas flaring and residential combustion emissions, Atmospheric Chemistry and Physics, 13, 8833-8855, https://doi.org/10.5194/acp-13-8833-2013, 2013.

Rienecker, M., Suarez, M. J., Todling, R., Bacmeister, J., Takacs, L., Liu, H., Gu, W., Sienkiewicz, M., Koster, R., Gelaro, R., Stajner, I., and Nielsen, J.: The GEOS-5 Data Assimilation System-Documentation of Versions 5.0. 1, 5.1. 0, and 5.2. 0, 2008.

Updyke, K. M., Nguyen, T. B., and Nizkorodov, S. A.: Formation of brown carbon via reactions of ammonia with secondary organic aerosols from biogenic and anthropogenic precursors, Atmospheric Environment, 63, 22-31, https://doi.org/10.1016/j.atmosenv.2012.09.012, 2012.

Wang, H., Easter, R. C., Rasch, P. J., Wang, M., Liu, X., Ghan, S. J., Qian, Y., Yoon, J.-H., Ma, P.-L., and Vinoj, V.: Sensitivity of remote aerosol distributions to representation of cloud–aerosol interactions in a global climate model, Geoscientific Model Development, 6, 765-782, https://doi.org/10.5194/gmd-6-765-2013, 2013.

Wang, M., Ghan, S., Easter, R., Ovchinnikov, M., Liu, X., Kassianov, E., Qian, Y., Gustafson Jr, W., Larson, V., and Schanen, D.: The multi-scale aerosol-climate model PNNL-MMF: Model description and evaluation, Geoscientific Model Development, 4, 137, https://doi.org/10.5194/gmd-4-137-2011, 2011.

Wang, X., Heald, C., Ridley, D., Schwarz, J., Spackman, J., Perring, A., Coe, H., Liu, D., and Clarke, A.: Exploiting simultaneous observational constraints on mass and absorption to estimate the global direct radiative forcing of black carbon and brown carbon, Atmospheric Chemistry and Physics, 14, 10989-11010, https://doi.org/10.5194/acp-14-10989-2014. 2014.

Wang, Q., Jacob, D.J., Spackman, J.R., Perring, A.E., Schwarz, J.P., Moteki, N., Marais, E.A., Ge, C., Wang, J. and Barrett, S.R.: Global budget and radiative forcing of black carbon aerosol: Constraints from pole-to-pole (HIPPO) observations across the Pacific. Journal of Geophysical Research: Atmospheres, 119(1), 195-206, https://doi.org/10.1002/2013JD020824, 2014.

Wang, X., Heald, C. L., Liu, J., Weber, R. J., Campuzano-Jost, P., Jimenez, J. L., Schwarz, J. P., and Perring, A. E.: Exploring the observational constraints on the simulation of brown carbon, Atmospheric Chemistry and Physics, 18, 635, https://doi.org/10.5194/acp-18-635-2018, 2018.

Ward, D. S., Kloster, S., Mahowald, N. M., Rogers, B. M., Randerson, J. T., and Hess, P. G.: The changing radiative forcing of fires: global model estimates for past, present and future, Atmospheric Chemistry and Physics, 12, 10857-10886, https://doi.org/10.5194/acp-12-10857-2012, 2012.

Washenfelder, R., Attwood, A., Brock, C., Guo, H., Xu, L., Weber, R., Ng, N., Allen, H., Ayres, B., and Baumann, K.: Biomass burning dominates brown carbon absorption in the rural southeastern United States, Geophysical Research Letters, 42, 653-664, https://doi.org/10.1002/2014GL062444, 2015.

Wofsy, S. C.: HIAPER Pole-to-Pole Observations (HIPPO): fine-grained, global-scale measurements of climatically important atmospheric gases and aerosols, Philosophical Transactions of the Royal Society of London A: Mathematical, Physical and Engineering Sciences, 369, 2073-2086, https://doi.org/10.1098/rsta.2010.0313, 2011.

Wong, J. P. S., Nenes. A., and Weber, R. J., Changes in light absorptivity of molecular weight separated brown carbon due to photolytic aging, Envir. Sci. Technol, 51, 8414-8421, https://doi.org/10.1021/acs.est.7b01739, 2017.

Wong, J. P. S., Tsgaraki, M., Tsiodra, I., Mihalopoulos, N., Vilaki, K., Kanakidou, M., Sciare, J., Nenes, A., and Weber, R. J., Atmospheric evolution of molecular weight separated brown carbon from biomass burning, Atm. Chem. Phys., 19, 7319-7334, https://doi.org/10.5194/acp-19-7319-2019 2019.

Xie, M., Hays, M. D., and Holder, A. L.: Light-absorbing organic carbon from prescribed and laboratory biomass burning and gasoline vehicle emissions, Scientific Reports, 7, 7318, https://doi.org/10.1038/s41598-017-06981-8, 2017.

Yan, C., Zheng, M., Bosch, C., Andersson, A., Desyaterik, Y., Sullivan, A. P., Collett, J. L., Zhao, B., Wang, S., and He, K.: Important fossil source contribution to brown carbon in Beijing during winter, Scientific Reports, 7, 43182, https://doi.org/10.1038/srep43182, 2017.

Yang, M., Howell, S., Zhuang, J., and Huebert, B.: Attribution of aerosol light absorption to black carbon, brown carbon, and dust in China–interpretations of atmospheric measurements during EAST-AIRE, Atmospheric Chemistry and Physics, 9, 2035-2050, https://doi.org/10.5194/acp-9-2035-2009, 2009.

Yoshimori, M., and Broccoli, A. J.: Equilibrium response of an atmosphere–mixed layer ocean model to different radiative forcing agents: Global and zonal mean response, Journal of Climate, 21, 4399-4423, https://doi.org/10.1175/2008JCLI2172.1, 2008.

Yu, L., Smith, J., Laskin, A., George, K. M., Anastasio, C., Laskin, J., Dillner, A. M., and Zhang, Q.: Molecular transformations of phenolic SOA during photochemical aging in the aqueous phase: competition among oligomerization, functionalization, and fragmentation, Atmospheric Chemistry and Physics, 16, 4511-4527, 2016.

Zhang, G., and McFarlane, N. A.: Sensitivity of climate simulations to the parameterization of cumulus convection in the Canadian Climate Centre general circulation model, Atmosphere-ocean, 33, 407-446, https://doi.org/10.1080/07055900.1995.9649539, 1995.

Zhang, Q., Streets, D. G., Carmichael, G. R., He, K., Huo, H., Kannari, A., Klimont, Z., Park, I., Reddy, S., and Fu, J.: Asian emissions in 2006 for the NASA INTEX-B mission, Atmospheric Chemistry and Physics, 9, 5131-5153, https://doi.org/10.5194/acp-9-5131-2009, 2009.

Zhang, X., Lin, Y. H., Surratt, J. D., Zotter, P., Prévôt, A. S., and Weber, R. J.: Light-absorbing soluble organic aerosol in Los Angeles and Atlanta: A contrast in secondary organic aerosol, Geophysical Research Letters, 38, https://doi.org/10.1029/2011GL049385, 2011.

Zhang, Y., Forrister, H., Liu, J., Dibb, J., Anderson, B., Schwarz, J. P., Perring, A. E., Jimenez, J. L., Campuzano-Jost, P., and Wang, Y.: Top-of-atmosphere radiative forcing affected by brown carbon in the upper troposphere, Nature Geoscience, 10, 486, https://doi.org/10.1038/ngeo2960, 2017.

Zhao, R., Lee, A., Huang, L., Li, X., Yang, F., and Abbatt, J.: Photochemical processing of aqueous atmospheric brown carbon, Atmospheric Chemistry and Physics, 15, 6087-6100, https://doi.org/10.5194/acp-15-6087-2015, 2015.

Zhong, M., and Jang, M.: Light absorption coefficient measurement of SOA using a UV–Visible spectrometer connected with an integrating sphere, Atmospheric environment, 45, 4263-4271, https://doi.org/10.1016/j.atmosenv.2011.04.082, 2011.

Zhong, M., Jang, M., Oliferenko, A., Pillai, G. G., and Katritzky, A. R.: The SOA formation model combined with semiempirical quantum chemistry for predicting UV-Vis absorption of secondary organic aerosols, Physical Chemistry Chemical Physics, 14, 9058-9066, https://doi.org/10.1039/c2cp23906j, 2012.

Zhou, Y., Xu, K. M., Sud, Y., and Betts, A.: Recent trends of the tropical hydrological cycle inferred from Global Precipitation Climatology Project and International Satellite Cloud Climatology Project data, Journal of Geophysical Research: Atmospheres, 116, https://doi.org/10.1029/2010JD015197, 2011.

Zou, Y., Wang, Y., Ke, Z., Tian, H., Yang, J., and Liu, Y.: Development of a REgion-Specific Ecosystem Feedback Fire (RESFire) Model in the Community Earth System Model, Journal of Advances in Modeling Earth Systems, 11, 417-445, https://doi.org/10.1029/2018MS001368, 2019.

785

For

Table 1. BrC emission sources (TgC yr^{-1}) of this and previous studies.

	This work	Jo et. al. (2016)	Wang et al. (2014)
Primary biomass burning source	3.6	3.0±1.7	8 for primary sources
Primary biofuel source	3.1	3.0±1.3	
Secondary formation	4.1	5.7	3.2

790

795 **Table 2. BrC sensitivity simulations**

CAM run name	NCNB (base model)	ICNB	NCB	ICBB	ICB (best model)
Reduced BrC convective wet scavenging	No	Yes	No	Yes	Yes
Photo-bleaching of convective transported BrC	No	No	Yes	Yes	No
Photo-bleaching of non- convective transported BrC	No	No	Yes	Yes	Yes

800

805

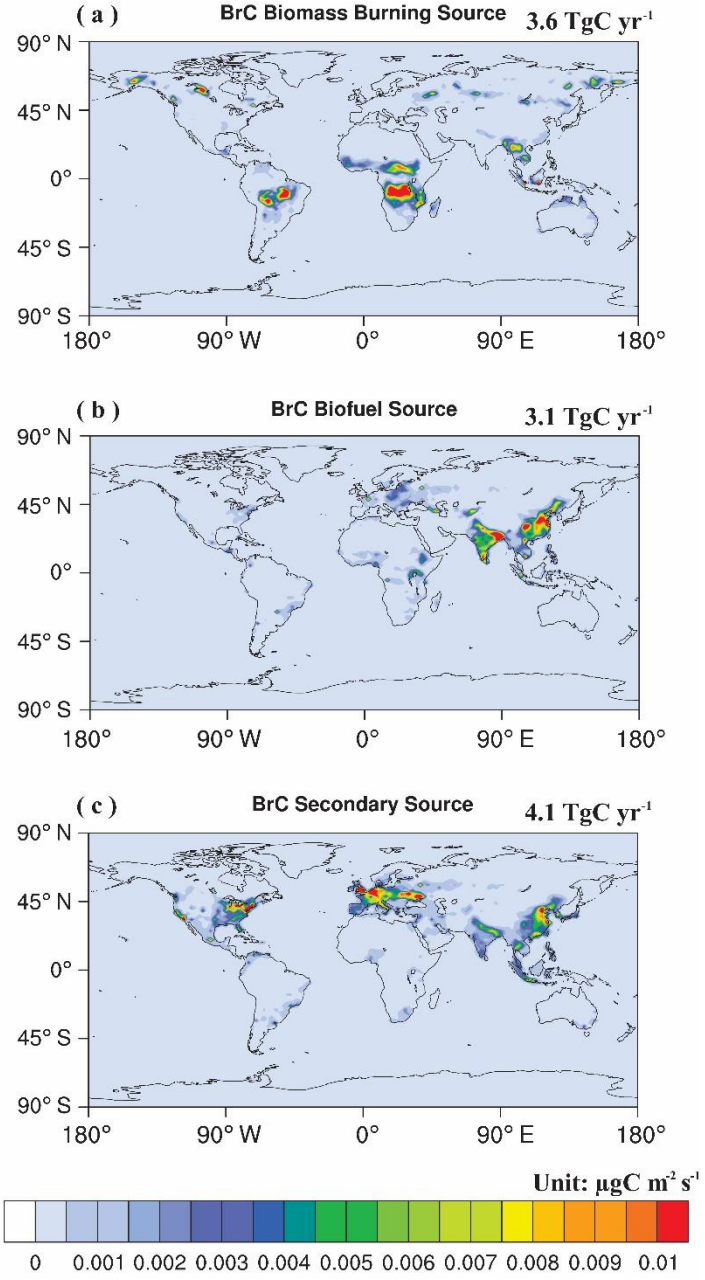

Figure 1. Spatial distributions of global emissions of BrC from biomass burning (a), anthropogenic biofuel combustion (b) and secondary formation (c) in 2010. Unit is μg C m^{-2} s^{-1}. The total emission is 3.6, 3.1, and 4.1 Tg C yr^{-1} for biomass burning, biofuel, and secondary formation, respectively.

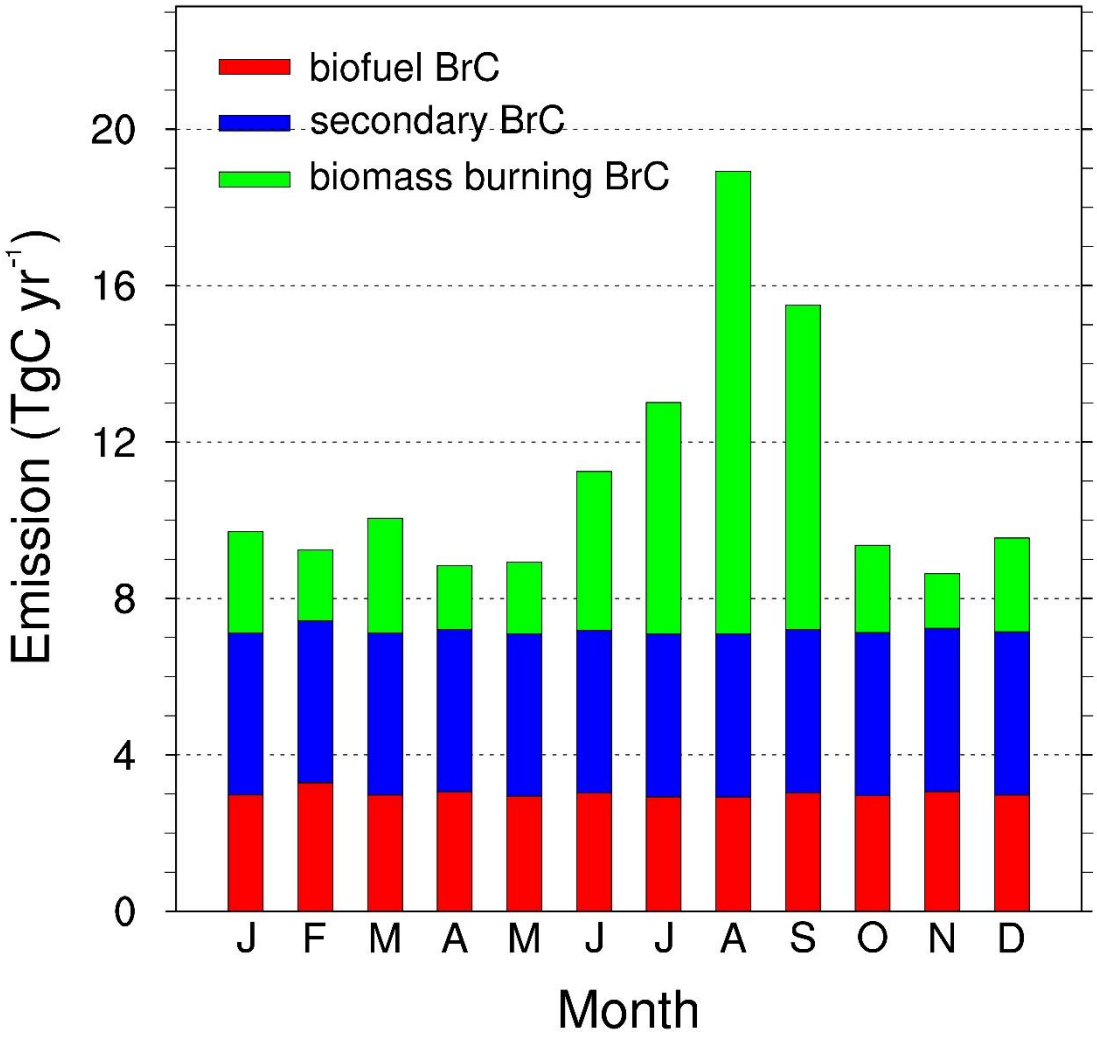

Figure 2. Monthly mean global BrC emission rates (Tg C yr^{-1}) in 2010. Green, blue, and red bars represent the emissions from biomass burning, biofuel combustion, and secondary BrC formation, respectively.

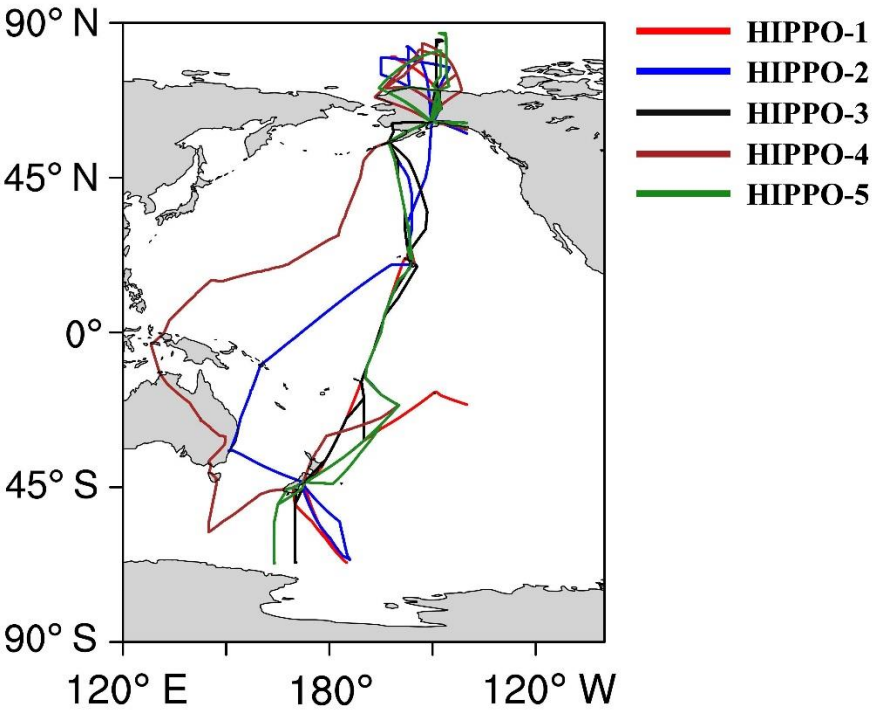

Figure 3. Flight track of the 5 HIPPO missions. Colored lines in red, blue, black, brown, green represent flight track of HIPPO-1 to HIPPO-5 respectively. Flights over continental North America east of 140°W were not included in this study.

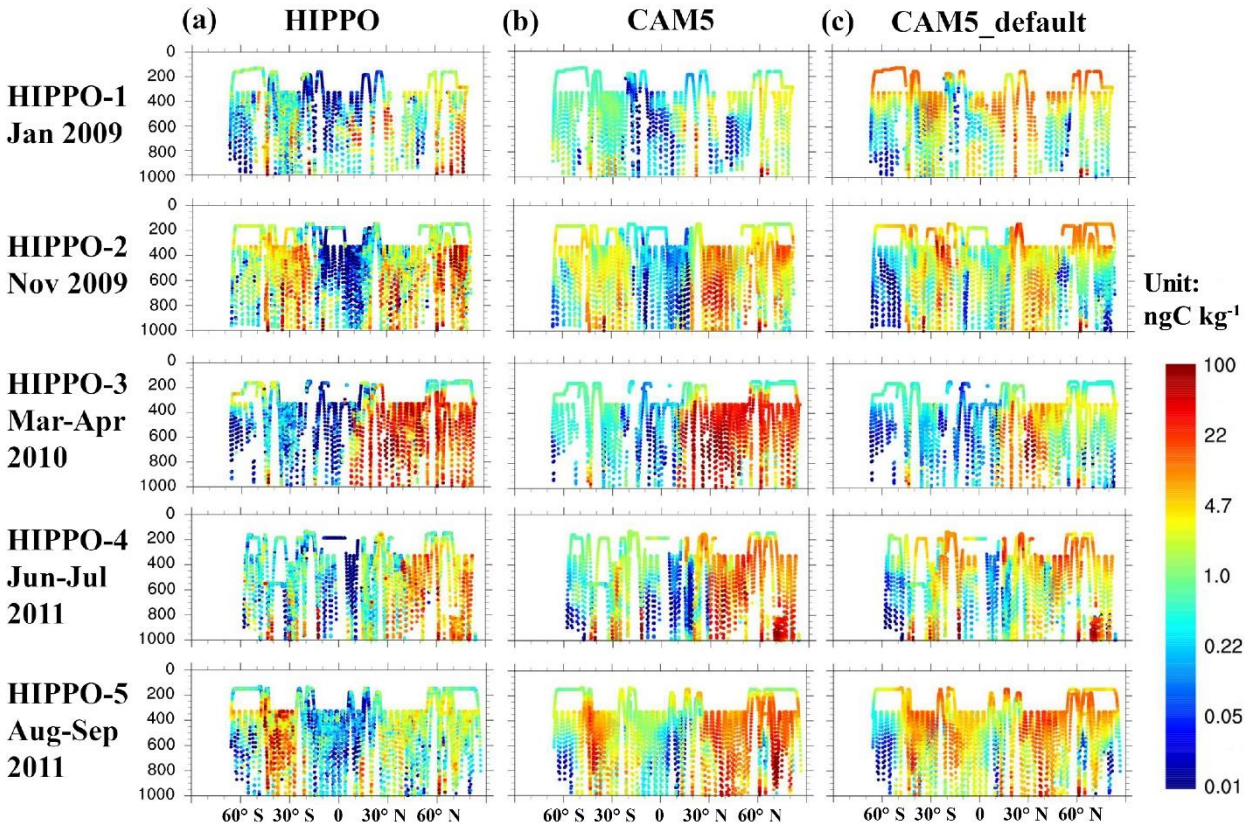

820 **Figure 4**. Comparison of HIPPO BC (ng C kg^{-1}) measurements (a), simulated BC data from the modified CAM5 model (b) and simulated BC data from the default CAM5 model (c) during HIPPO mission 1-5. The 5 rows from top to bottom are HIPPO-1 (Jan 2009), HIPPO-2 (Nov, 2009), HIPPO-3 (Mar-Apr, 2010), HIPPO-4 (Jun-Jul, 2011), and HIPPO-5 (Aug-Sep, 2011), respectively. Measurement data along the flight tracks of Fig. 3 are 1-min averages. Model data are selected corresponding to the location and time of aircraft measurements.

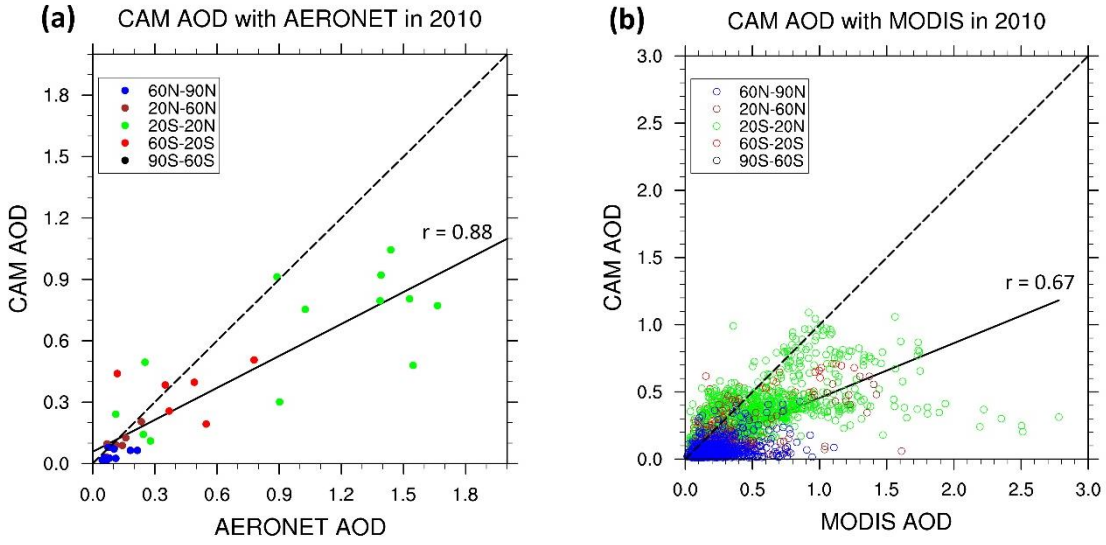

825

Figure 5. Comparison of monthly mean AOD data in 550 nm for fire dominated months and regions (Figure S1(a)) of model simulations with observations for 2010, (a) AERONET and (b) MODIS. Model data correspond to the same time and location of the observations. The data points are color-coded as a function of latitude. The solid line denotes a least-squares regression and the dashed line denotes the 1:1 reference line.

830

835

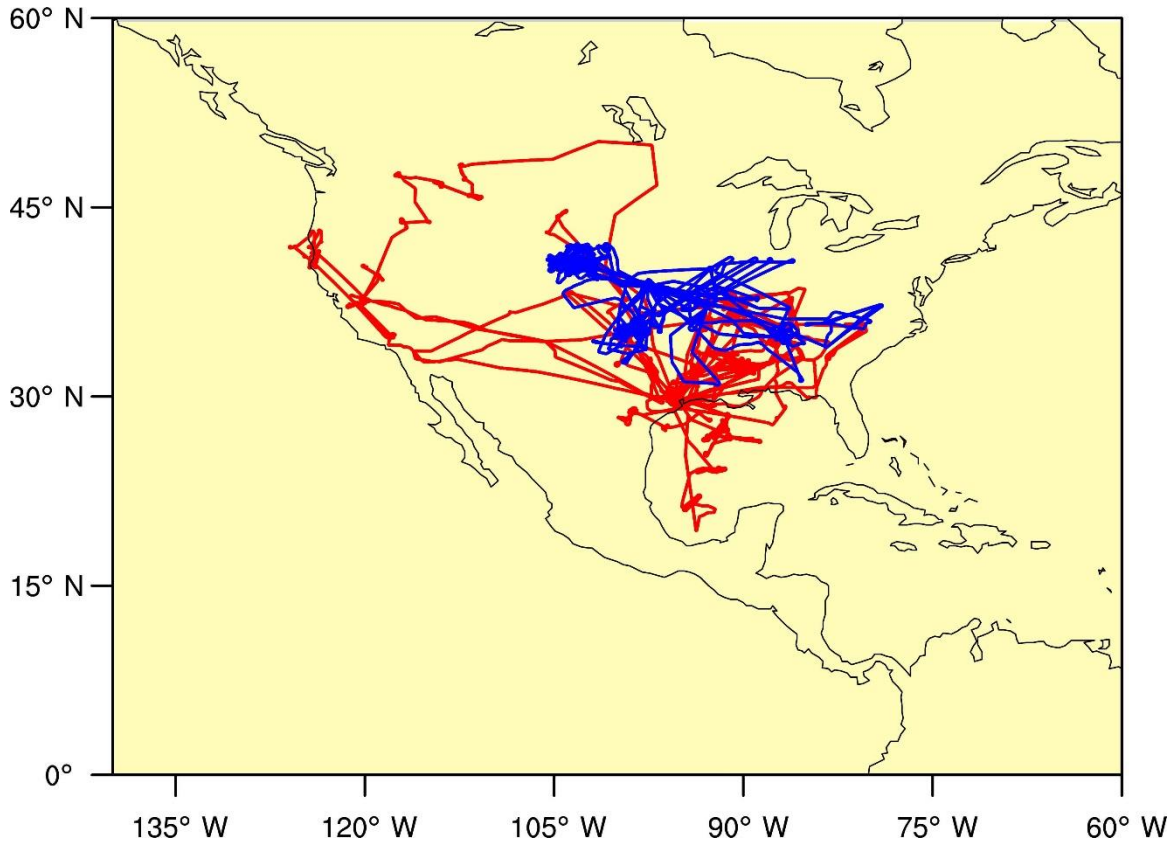

840 **Figure 6**. Flight tracks of DC3 (red) and SEAC^{4}RS (blue) field experiments.

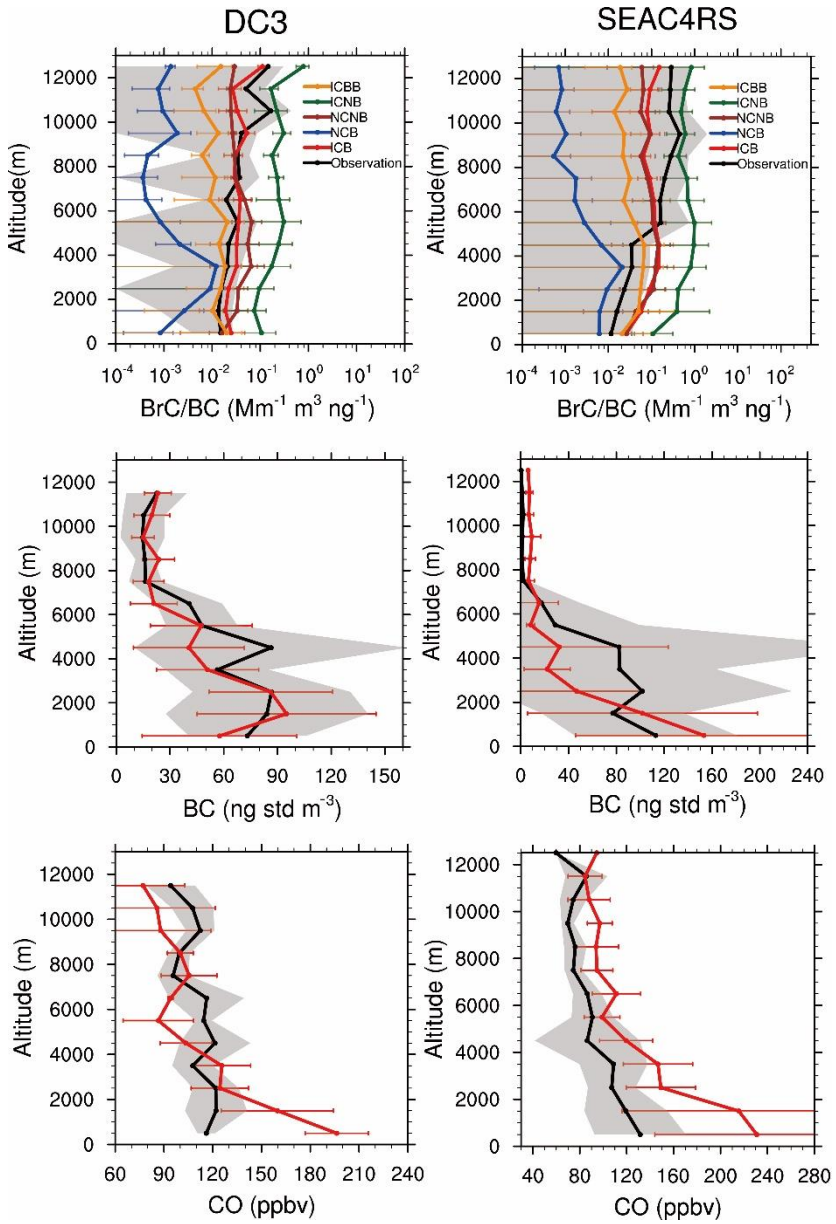

Figure 7. Comparison between observed and simulated vertical profiles of the ratio between BrC absorption at 365 nm and BC (top), and concentrations of BC (middle) and CO (bottom) for the DC3 (left column) and SEAC^{4}RS (right column) missions. Black lines and shaded areas show the means and standard deviations of the observations binned in 1-km intervals, respectively. The colored vertical lines and horizontal bars show the means and standard deviations of corresponding model results, respectively. Model sensitivity simulations of BrC are listed in Table 2. The difference among simulated BC and CO vertical profiles is negligible and the ICB simulation results are shown.

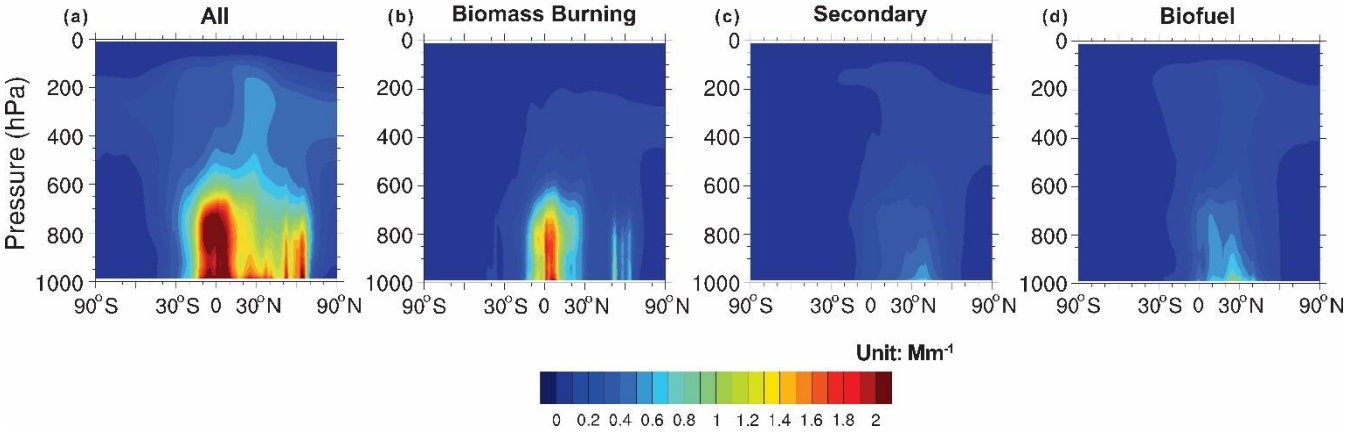

Figure 8. Simulated zonal averaged annual mean BrC absorption at 365 nm (Mm^{-1}) for (a) all sources, (b) biomass burning emissions, (c) secondary BrC formation, and (d) biofuel BrC emissions. Unit is Mm^{-1}. Color bar is in log scale.

855

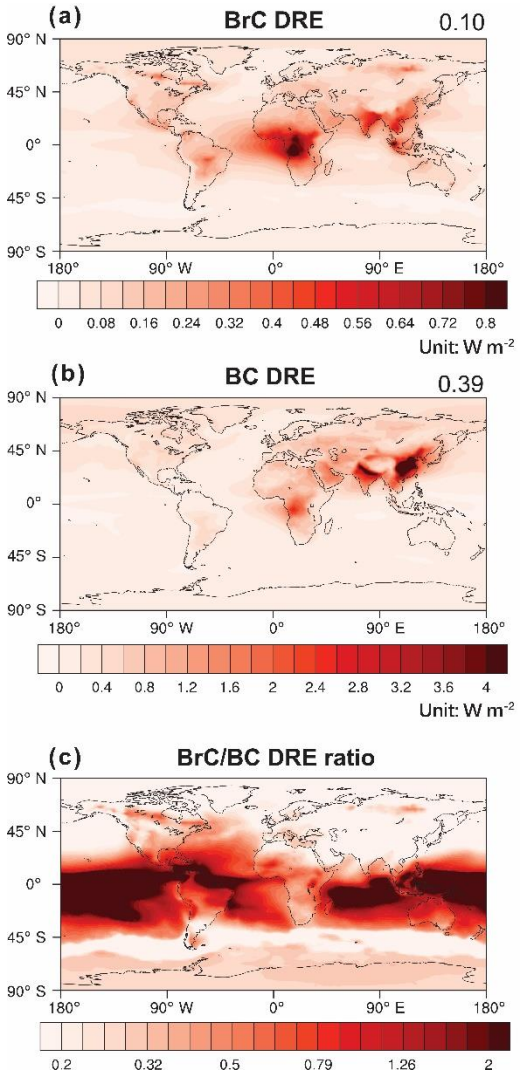

Figure 9. Annual averaged global distributions of (a) BC DRE, (b) BrC DRE, and (c) ratio of BrC/BC DRE for 2010. The unit is W m^{-2}. The global averaged DRE is shown in the upper right corner.

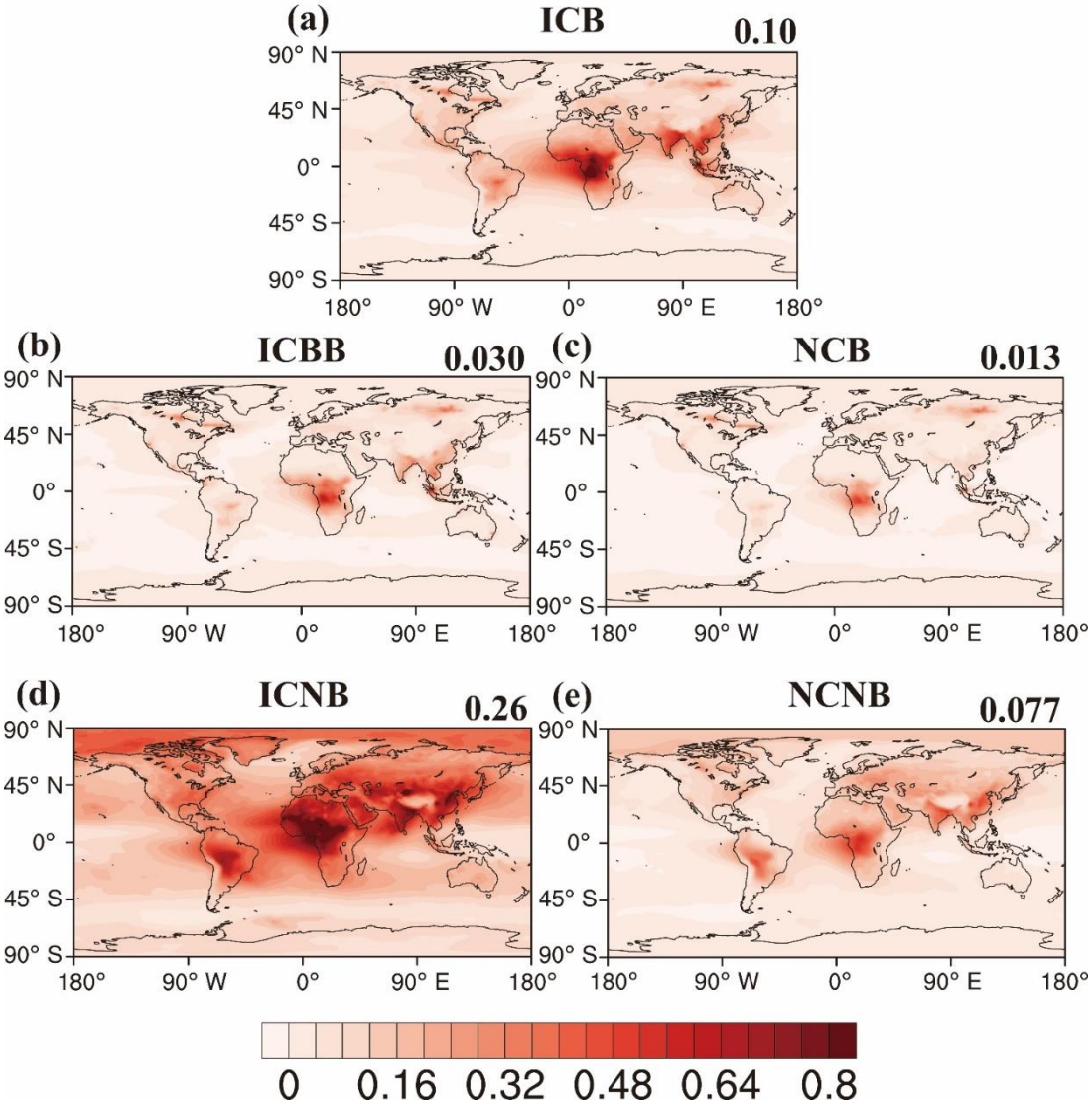

Figure 10. Annual averaged global distributions of BrC DRE for all sensitivity simulations (Table 2). The unit is W m^{-2}. The global averaged DRE is shown in the upper right corner.

860

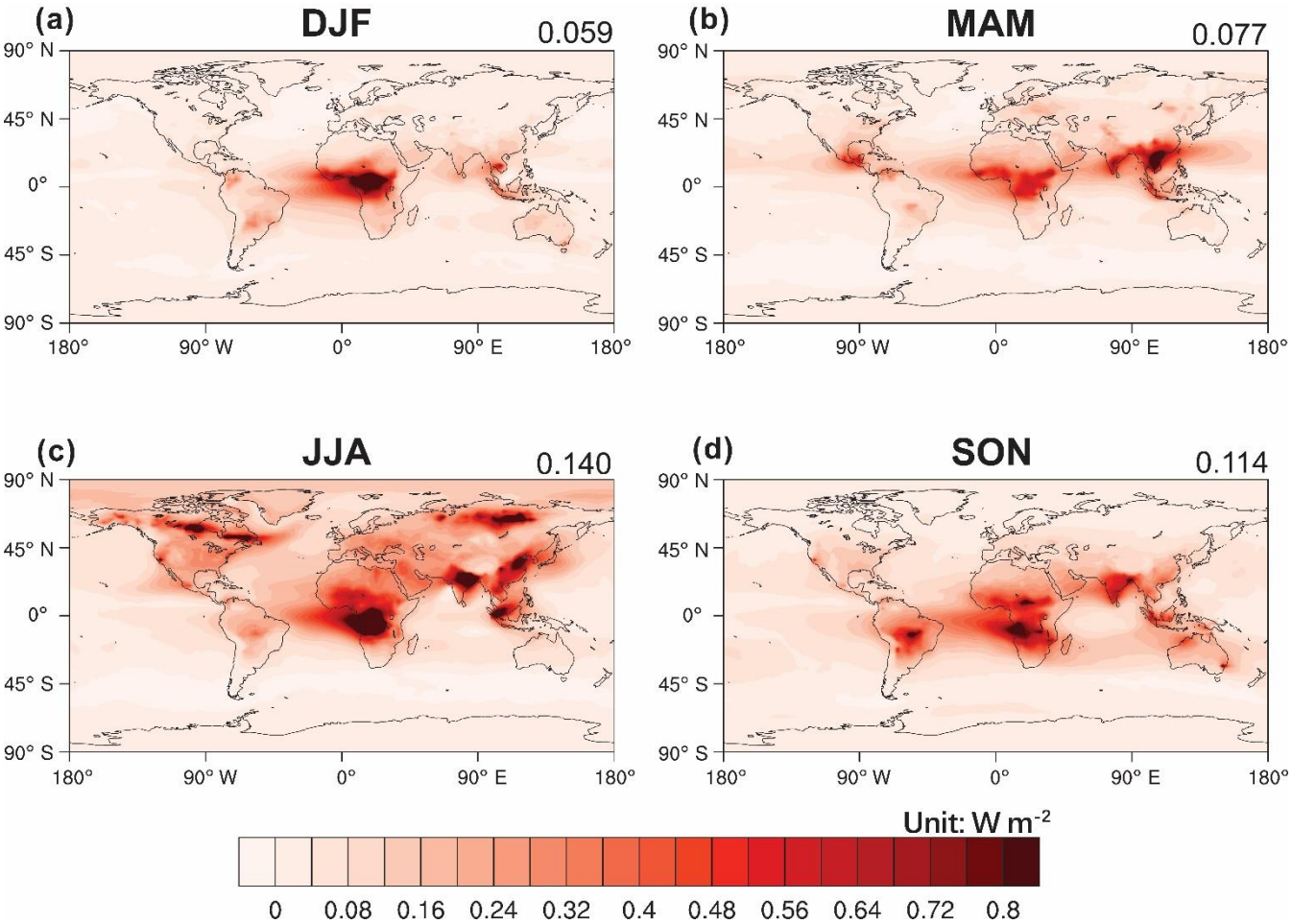

Figure 11. Same as Fig. 10 but for seasonal global DRE distributions of BrC for (a) DJF, (b) MAM, (c) JJA, (d) SON in the ICB simulation.

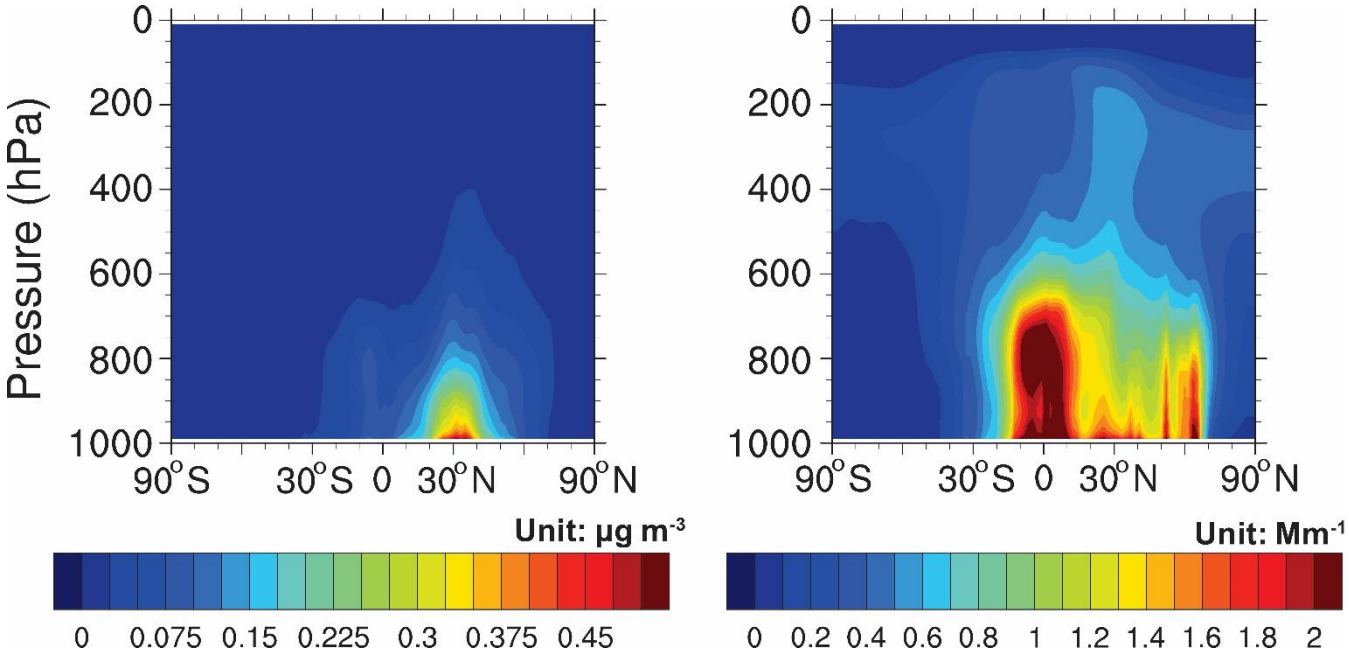

Figure 12. Global zonal mean distributions of (a) BC mass concentrations (μg std m^{-3}) and (b) BrC absorption at 365 nm (Mm^{-1}) for 2010.

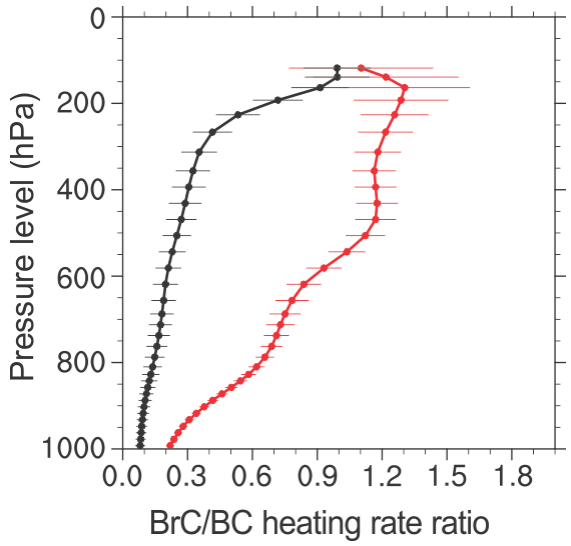

Figure 13. Global averaged vertical profile of BrC toBC heating rate ratio for 2010. The black and red lines are the average profiles for regions without and with deep convection events, respectively. Standard deviations are indicated by the horizontal bars.

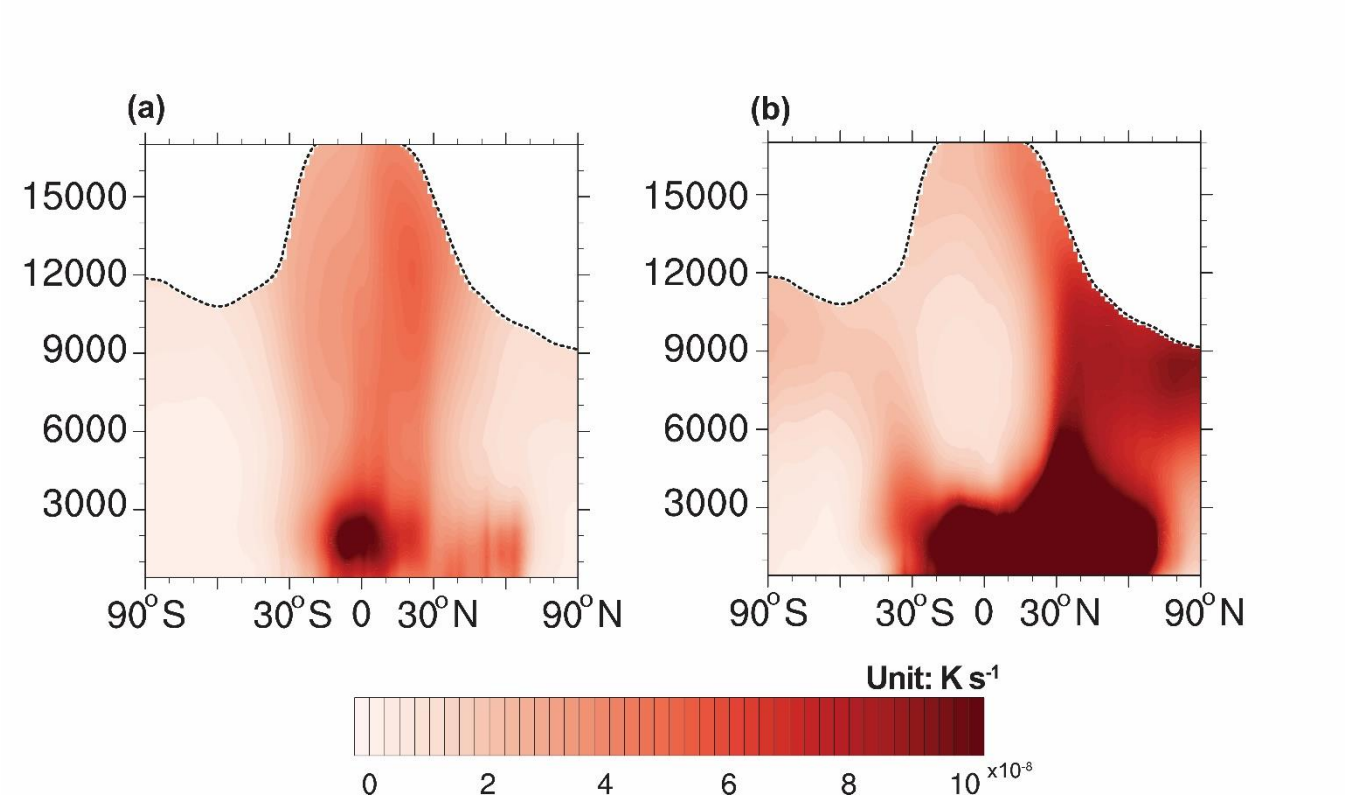

875

Figure 14. Global zonal mean distributions of heating rate of (a) BrC and (b) BC for 5 years of present-day simulations. The dash line denotes the tropopause.

880

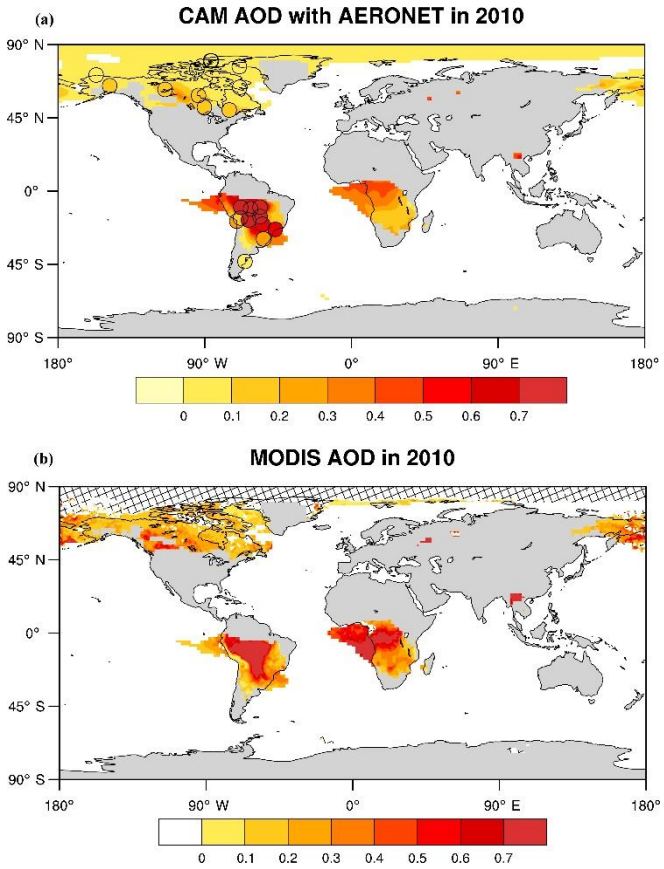

Figure S1. Simulated (a) and MODIS observed (b) 550 nm AOD data averaged for the months and regions in which fire emissions account for < 50% of the total AOD for 2010. AERONET measurements in the corresponding months and regions are shown as color-coded open circles in (a). MODIS data in the shaded Arctic region in (b) are not used due to the uncertainty of MODIS retrieval above bright surface (Remer et al., 2013).

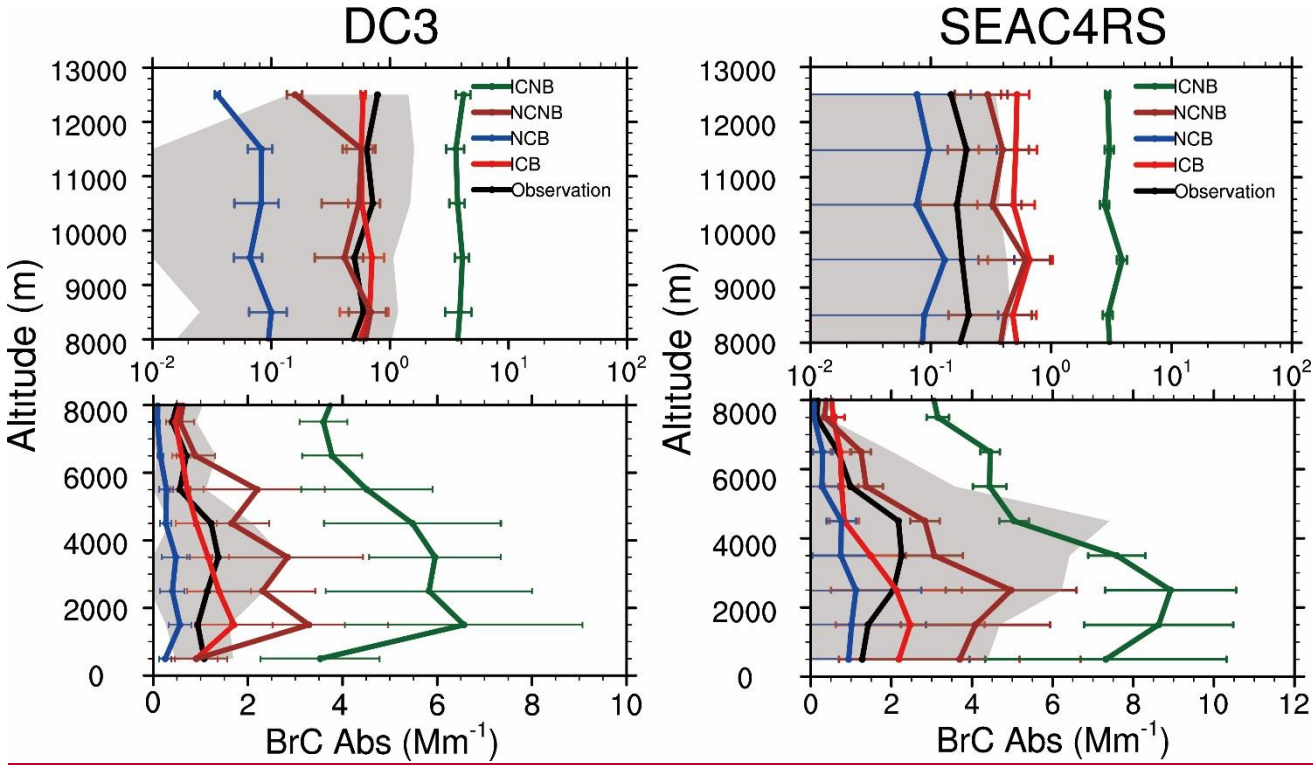

Figure S2. Comparison between observed and simulated vertical profiles of BrC absorption at 365 nm. Black lines and shaded areas show the means and standard deviations of the observations binned in 1-km intervals, respectively. The colored vertical lines and horizontal bars show the means and standard deviations of corresponding model results, respectively. Model sensitivity simulations of BrC are listed in Table 2.

Table S1a. RRTMG wavelength boundaries for shortwave

Band Index	Lower boundary Wavelength (nm)	Upper Boundary Wavelength (nm)
1	3077	3846
2	2500	3077
3	2150	2500
4	1942	2150

5	1626	1942
6	1299	1626
7	1242	1299
8	778	1242
9	625	778
10	442	625
11	345	442
12	263	345
13	200	263

Table S1b. RRTMG wavelength boundaries for longwave

Band Index	Lower boundary Wavelength (μm)	Upper Boundary Wavelength (μm)
1	28.57	1000
2	20	28.57
3	15.87	20
4	14.29	15.87
5	12.2	14.29
6	10.2	12.2
7	9.26	10.2
8	8.47	9.26
9	7.19	8.47
10	6.76	7.19
11	5.56	6.76
12	4.81	5.56
13	4.44	4.81
14	4.2	4.44
15	3.85	4.2
16	3.08	3.85

Reference

Remer, L., Mattoo, S., Levy, R., and Munchak, L.: MODIS 3 km aerosol product: algorithm and global perspective, Atmospheric Measurement Techniques, 6, 1829, 2013.